

ÜFLEMELİ SES ÜSTÜ RÜZGAR TÜNELİ ÖN TASARIMI

Kadir Giray KUYUMCU

YÜKSEK LİSANS TEZİ

SAVUNMA TEKNOLOJİLERİ ANA BİLİM DALI

SİVAS BİLİM VE TEKNOLOJİ ÜNİVERSİTESİ

LİSANSÜSTÜ EĞİTİM ENSTİTÜSÜ

ŞUBAT 2024

ETİK BEYAN

Sivas Bilim ve Teknoloji Üniversitesi Lisansüstü Eğitim Enstitüsü Tez Yazım Kurallarına uygun olarak hazırladığım bu tez çalışmada;

- Tez içinde sunduğum verileri, bilgileri ve dokümanları akademik ve etik kurallar çerçevesinde elde ettiğimi,
 - Tüm bilgi, belge, değerlendirme ve sonuçları bilimsel etik ve ahlak kurallarına uygun olarak sunduğumu,
 - Tez çalışmada yararlandığım eserlerin tümüne uygun atıfta bulunarak kaynak gösterdiğimi,
 - Kullanılan verilerde herhangi bir değişiklik yapmadığımı,
 - Bu tezde sunduğum çalışmanın özgün olduğunu,
- bildirir, aksi bir durumda aleyhime doğabilecek tüm hak kayıplarını kabullendiğimi beyan ederim.

.....
Kadir Giray KUYUMCU
01/02/2024

ÜFLEMELİ SES ÜSTÜ RÜZGAR TÜNELİ ÖN TASARIMI

(Yüksek Lisans Tezi)

Kadir Giray KUYUMCU

SİVAS BİLİM ve TEKNOLOJİ ÜNİVERSİTESİ

LİSANSÜSTÜ EĞİTİM ENSTİTÜSÜ

Şubat 2024

ÖZET

Bu çalışmada orta ölçekli bir ses üstü üflemeli rüzgar tüneli için ön tasarım sunulmaktadır. Test bölümünün kesit boyutları, 0,4 m x 0,4 m olarak belirlenmiştir ve hedeflenen maksimum hız Mach 4'tür. Düşük maliyeti ve değişen Reynolds sayılarında çalışma kabiliyeti nedeniyle, "blowdown" tünel tipi seçilmiştir. İlk tahminler, Mach 4'te 60 saniyelik bir çalışma süresini belirlemek için yapılmıştır. Mach 4'te tüneli başlatmak için gereken giriş basıncı, çıkış basıncının deniz seviyesinde atmosfer basıncına eşit olduğu varsayılarak yaklaşık 15 bar olarak hesaplanmıştır. Mach 4'te 60 saniyelik bir deneyi mümkün kılmak için, maksimum sıkıştırma kapasitesi 40 bar olan bir kompresör ve toplam kapasiteleri 40 m³ olan basınç tankları seçilmiştir. Tünelin nozul "nozzle" geometrisini oluşturmak için "Method of Characteristics" kullanılmıştır. MATLAB yazılımı kullanılarak bu yöntem uygulanmış ve farklı parametrelere bağlı olarak nozul geometrisi oluşturabilecek bir kod hazırlanmıştır, MoC'den elde edilen koordinatlar, bir bilgisayar destekli çizim yazılımına aktararak nozul geometrisi oluşturulmuştur. Son olarak, ANSYS Fluent 2023 R1 yazılımı kullanılarak 2-boyutlu ve 3-boyutlu CFD yöntemi ile nozul geometrisi doğrulanmış ve ağ bağımlılığı "mesh dependency" çalışması yapılmıştır. Tüm bu süreç, çözümün doğruluğunu kontrol edebilmek için Mach 2 hızında tekrarlanmıştır. CFD analizi sonuçları, nozulun çıkış bölümündeki Mach sayısı düzgünlüğünün tatmin edici olduğunu göstermektedir.

Bilim Kodu : 93107

Anahtar Kelimeler : Üflemeli Ses Üstü Rüzgar Tüneli, Deneysel Aerodinamik, Hesaplamalı Akışkanlar Dinamiği, Mach Sayısı

Sayfa Adedi : 43

Danışman : Dr. Öğr. Üyesi Yaşar OSTOVAN

PRELIMINARY DESIGN OF AN INTERMITTENT BLOWDOWN SUPERSONIC
WIND TUNNEL

(M. Sc. Thesis)

Kadir Giray KUYUMCU

SİVAS UNIVERSITY OF SCIENCE AND TECHNOLOGY
INSTITUTE OF GRADUATE STUDIES

February 2024

ABSTRACT

The preliminary design for a mid-scale supersonic blowdown wind tunnel is presented in this study. The cross-sectional dimensions of the test section are determined to be 0,4 m by 0,4 m, and Mach 4 is the target maximum operational speed of the wind tunnel. The blowdown intermittent tunnel type was selected due to comparatively low built costs and its ability to operate at varying Reynolds numbers. First estimates are made in order to determine a run time of 60 seconds at Mach 4. The required inlet pressure to start the tunnel at Mach 4 is calculated to be roughly 15 bars, assuming that the output pressure is equal to atmospheric pressure at sea level. To enable a 60-second run time at Mach 4, a compressor with a maximum compression capacity of 40 bars feeding a series of tanks with total volumetric capacity of 40 m^3 are chosen. The Method of Characteristics is implemented to develop the converging diverging nozzle geometry utilizing a code developed in MATLAB. Nozzle geometry is constructed by importing the contours' coordinates provided by the MoC approach into a computer-aided design program. Moreover, ANSYS Fluent 2023 R1 is used to confirm the nozzle geometry through both two-dimensional and three-dimensional CFD analyses. Meanwhile, mesh dependency study is performed to optimize the CFD analyses setup. The whole process is repeated for a different Mach number, Mach 2, to validate the methodology. The CFD study results indicate that there exists acceptable Mach number distribution uniformity at the exit border of the nozzles for both Mach 2 and Mach 4.

Science Code : 93107

Key Words : Supersonic Blowdown Wind Tunnels, Experimental Aerodynamics,
Computational Fluid Dynamics, Mach Number

Page Number : 43

Supervisor : Asst. Prof. Dr. Yaşar OSTOVAN

TEŐEKKÖR

Yıllar boyunca ciddi bir uğraő ve özveri ile hazırladığım yüksek lisans tezimi tamamlamanın heyecanını ve gururunu yaşıyorum.

Bu çalışmanın hayata geçirilmesi sürecinde bilgi ve tecrübelerinden faydalandığım danışman hocam Dr. Öğretim Üyesi Yaşar OSTOVAN'a, araőtırmalarımın her bir aşamasında görüşleriyle beni destekleyen fakülte hocalarıma, bu süreçte her konuda fikirlerini ve yardımlarını benden esirgemeyen çalışma arkadaşlarıma, değerli arkadaşım Aşşenur Öztürk'e ve son olarak hayatım boyunca aldığım her kararında arkamda olan, maddi ve manevi desteklerini hiçbir zaman esirgemeyen aile üyelerime teşekkür ederim.



CONTENTS

	Page
ÖZET	iv
ABSTRACT.....	v
TEŞEKKÜR.....	vi
LIST OF TABLES	viii
LIST OF FIGURES	ix
SYMBOLS AND ABBREVIATIONS.....	xii
1. INTRODUCTION.....	1
2. METHODOLOGY	8
2.1. Nozzle Design	12
2.1.1. The Method of Characteristics	13
2.2. CFD Analysis	17
3. CFD SIMULATIONS RESULTS AND DISCUSSION	18
3.1. Y+ Estimation	18
3.2. Mesh Dependency	20
3.3. Boundary Conditions & Initial Conditions	20
3.4. 2D CFD Analysis	21
3.5. Mesh Dependency on Boundary Layer	27
3.6. 3D CFD Analysis	29
3.7. Comparison of 2D and 3D CFD Analysis.....	35
4. CONCLUSION	37
REFERENCES	39

LIST OF TABLES

Table	Page
Table 1.1. Supersonic & Trisomic wind tunnels.....	6
Table 1.1. (continued) Supersonic & Trisomic wind tunnels	7
Table 2.1. Run times vs. Mach number	10
Table 3.1.1. Y+ Calculation inputs for Mach 4	19
Table 3.1.2. Y+ Calculation inputs for Mach 2	19
Table 3.4.1. Mesh dependency study of 2D model for Mach 4.....	21
Table 3.4.2. Mesh dependency study of 2D model for Mach 2.....	21
Table 3.6.1. Mesh statistics for 3D model for Mach 2	29
Table 3.6.2. Mesh statistics for 3D model for Mach 4	31

LIST OF FIGURES

Figure	Page
Figure 1.1. Schematic view of a supersonic wind tunnel	3
Figure 1.2. Schematic view of pressure regulator.....	3
Figure 1.3. Nozzle geometry.....	4
Figure 1.4. Forces and moments acting on the model under test.....	5
Figure 1.5. General view of diffuser geometry.....	5
Figure 2.1. Flowchart of the study	8
Figure 2.2. Schematic of the main components of a supersonic blow-down wind tunnel ...	9
Figure 2.3. Run time vs Mach number	11
Figure 2.4. Mach Number vs. tunnel compression ratio [3]	11
Figure 2.5. Gradual-expansion nozzle (left) vs minimum length nozzle (right)	12
Figure 2.1.1. Gradual expansion of supersonic flow [22].....	13
Figure 2.1.2. Design procedure of nozzle geometry [23]	14
Figure 2.1.3. Mach 2 nozzle contour	15
Figure 2.1.4. Mach 4 nozzle contour	16
Figure 2.1.5. Mach 4 nozzle geometry	16
Figure 2.1.6. Mach 2 nozzle geometry	16
Figure 3.4.1. Close view of surface mesh.....	22
Figure 3.4.2. Mach number contour from the Fluent simulation of the Mach 4 nozzle geometry.....	22
Figure 3.4.3. Mach 4 geometry velocity contour of the boundary layer	23
Figure 3.4.4. Mach number contour from the Fluent simulation of the Mach 2 nozzle geometry.....	23
Figure 3.4.5. Mach 2 geometry velocity contour of the boundary layer	23

Figure	Page
Figure 3.4.6. Surface pressure distribution for Mach 4 nozzle	24
Figure 3.4.7. Surface pressure distribution for Mach 2 nozzle	24
Figure 3.4.8. Mach number vertical distribution in the outlet of the nozzle for different mesh numbers (in millions) (Mach 4)	24
Figure 3.4.9. Mach number vertical distribution in the outlet of the nozzle for different mesh numbers (in millions) in a close range (Mach 4)	25
Figure 3.4.10. Mach number vertical distribution in the outlet of the nozzle for different mesh numbers (in millions) in a close range for Mach 2	25
Figure 3.4.11. Mach 2 nozzle mesh convergence study (2d).....	26
Figure 3.4.12. Mach 4 nozzle mesh convergence study (2d).....	26
Figure 3.4.13. Mach 2 nozzle mesh convergence plot (2d – 4m mesh)	27
Figure 3.4.14. Mach 4 nozzle mesh convergence plot (2d – 4m mesh)	27
Figure 3.5.1: Mach number distribution at the boundary layer for different Mesh numbers (in millions) (Mach 2).....	28
Figure 3.5.2: Mach number distribution at the boundary layer for different mesh numbers (in millions) (Mach 4).....	28
Figure 3.6.1. Mach number contours for 3D CFD analysis of Mach 2	30
Figure 3.6.2. Mach number contours for 3D CFD analysis of Mach 2 (mid-plane)	30
Figure 3.6.3. Mach number vertical distribution in the outlet of the nozzle for different mesh numbers (in millions) for 3D CFD analysis (2 Mach)	31
Figure 3.6.4. Mach number vertical distribution in the outlet of the nozzle for different mesh numbers (in millions) in a close range for 3D CFD analysis (2 Mach)	31
Figure 3.6.5. Mach number contours for 3D CFD analysis of Mach 4	32
Figure 3.6.6. Mach number contours for 3D CFD analysis of Mach 4 (mid-plane)	32
Figure 3.6.7. Mach number vertical distribution in the outlet of the nozzle for different mesh numbers (in millions) for 3D CFD analysis (4 Mach)	32
Figure 3.6.8. Mach number vertical distribution in the outlet of the nozzle for different mesh numbers (in millions) in a close range for 3D CFD analysis (4 Mach)	33

Figure	Page
Figure 3.6.9. Mach 2 nozzle mesh convergency study (3d)	33
Figure 3.6.10. Mach 4 nozzle mesh convergency study (3d)	34
Figure 3.6.11. Mach 4 nozzle mesh convergence plot (3d – 12m mesh)	34
Figure 3.6.12. Mach 2 nozzle mesh convergence plot (3d – 8m mesh)	35
Figure 3.7.1. Comparison of 2D and 3D CFD analysis (Mach 2)	35
Figure 3.7.2. Comparison of 2D and 3D CFD analysis (Mach 4)	36



SYMBOLS AND ABBREVIATIONS

The symbols and abbreviations used in this study are presented below along with their explanations.

Symbols	Descriptions
a	Speed of sound
A	Area
c_f	Skin friction coefficient
h	Wall distance
M	Mach number
P	Pressure
R	Gas constant
Re	Reynolds Number
T	Temperature
U	Velocity
γ	Specific heat ratio
μ	Mach angle
ρ	Density
τ	Shear stress
ν	Prandtl-Meyer angle
Abbreviations	Descriptions
AR	Aspect Ratio
CFD	Computational Fluid Dynamics
MoC	Method of Characteristics
SST	Shear Stress Transport

1. INTRODUCTION

Wind tunnels are used to study the interaction of an object in contact with a moving fluid (generally air). They are utilized to test scaled models in a free stream flow provided under controlled conditions as if they are flying in real conditions [1]. Wind tunnel tests are widely used in fluid dynamics researches especially in aerospace applications. High-speed air vehicles that can reach supersonic conditions need these tests more due to their high cost and difficulty of testing in real conditions.

The main difference between low-speed testing and high-speed testing is compressibility of the air. In contrast to incompressible flow, where the fluid's density remains constant, compressible flow is commonly defined as variable density flow [2]. Based on configuration variations and their operational Mach number, wind tunnels can be classified into several groups. They can be categorized as subsonic ($M < 0.8$), transonic ($0.8 < M < 1.2$), supersonic ($1.2 < M < 5$) or hypersonic ($M > 5$) wind tunnels based on their operating Mach number. The tunnels can be either continuous or intermittent type depending on their configuration [3, 4].

Continuous type tunnels allow more control of conditions to the users. And also, users can provide stable testing conditions for a longer period of time [3]. Intermittent type supersonic wind tunnels have several advantages over continuous type such as ease of installation, lower cost and etc. [5]. Also, due to lower setup time, it is more convenient for model testing. Moreover, by comparing blow-down and indraft tunnels, blowdown type is more common as it allows to vary the Reynolds number widely at a particular Mach Number [3]. Considering all the advantages and disadvantages, blow-down intermittent type wind tunnels are the most commonly used type comparing the others. In this type of tunnel, the air does not circulate in the system and is released into the atmosphere from the outlet of the diffuser. Figure 1.1 presents a schematic of a blow-down supersonic wind tunnel and its main components.

Creating a steady, uniform flow in the test section over a range of Reynolds numbers is the primary objective of design a wind tunnel. The Reynolds number (Re), can be defined as the relationship between a typical inertial force and a typical viscous force and strongly influences the behavior of boundary layers, is the most important dimensionless group for tunnel design [4].

A stream of supersonic flow can be generated in a variety of ways, but the most typical method is to expand the test gas from a high-pressure reservoir via a nozzle to the appropriate Mach number [5]. Pressurized air is supplied from a compressor and there are several types of compressors that may be used to fill the storage tanks of a blowdown wind tunnel, but the piston compressor is by far the most popular, owing to its low cost and wide availability in a variety of sizes [6]. The pressure regulator is a high-frequency response valve to allow necessary pressure to start the tunnel and then regulate the flow rate to the desired operating conditions. In the settling chamber, the airflow becomes uniform utilizing flow straighteners upstream the nozzle. Then in the nozzle throat, the flow accelerates from subsonic speed to the desired supersonic speed and enters the test section. In addition to flow straighteners, nozzle geometry (contour) plays a crucial role to obtain a uniform flow inside the test section. The expansion duct or "diffuser" downstream of the working section is designed to slow down the flow [4]. Finally, a silencer is utilized to minimize the sound level of the system [7]. Figure 1.1 illustrates the schematic view of a supersonic wind tunnel.

Compressors are devices that supply air to the storage tank. Filling times vary depending on the capacity of the compressor and the volume of the tank. The air directed by the compressor passes through the dryer before it reaches the tank and the humidity decreases. The high humidity value of the air in the tunnel is a situation that significantly affects the test conditions. The air moving through the tunnel -if the humidity is not low- will start to condense in the test section by cooling down. Condensation will prevent reaching the desired speed value in the test section, but will cause a fog to seriously affect the imaging and measurements. For this reason, the air that will flow in the tunnel must be dried.

The pressure tank supplies compressed air to feed the airline. The volume of the tank is determined depending on the operation time. Tunnel run time is determined by considering the type and amount of data required during a particular run.

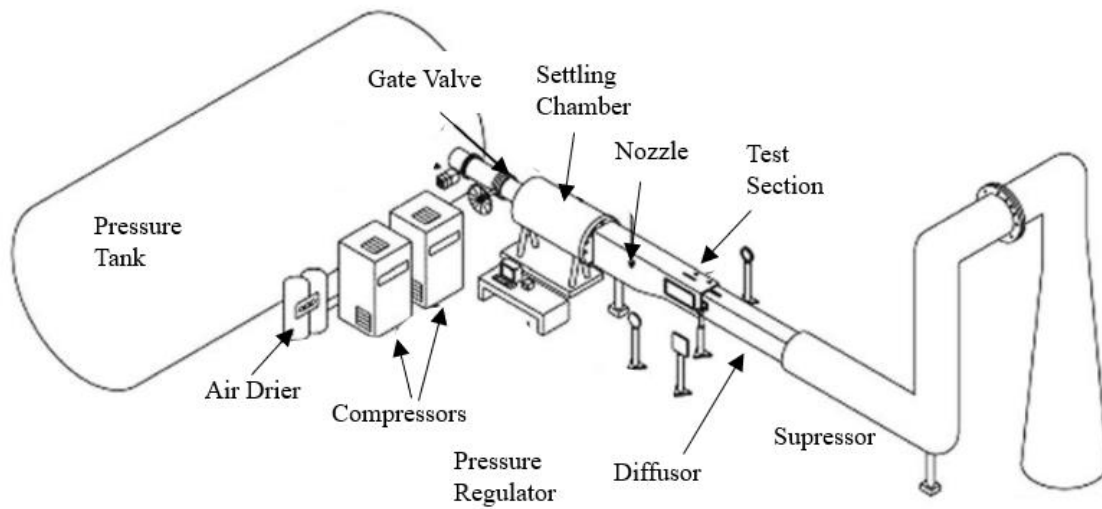


Figure 1.1. Schematic view of a supersonic wind tunnel

Gate valve is essentially a valve on which a plate is slid across the flow passage of the pipe. In the closed position, the sealing surfaces on the plate and valve body are forced into close contact with the pressure difference. When it is turned on, it allows air passage to the system. Almost often, wind tunnels are built to run at a steady stagnation pressure during any particular operation. A unique valve called the pressure control valve, which is depicted in Figure 1.2, is used to lower the available pressure in the storage tank while maintaining a steady wind tunnel stagnation pressure.

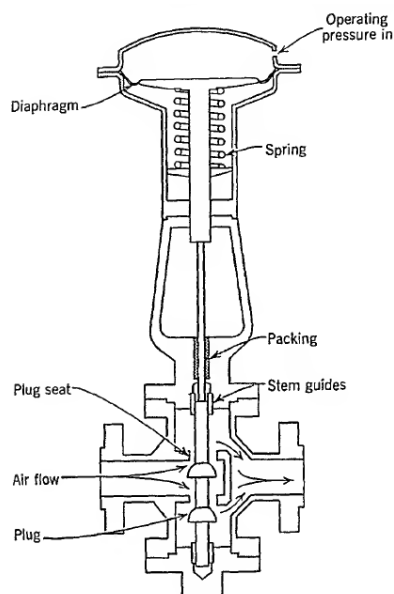


Figure 1.2. Schematic view of pressure regulator

The air from the wide-angle diffuser enters the settling chamber, which usually consists of a cylindrical shell with one diameter or more. Its length helps to produce uniform flow and lowers air turbulence. After the settling chamber, the air settles in the subsonic part (inlet) of the "nozzle" section.

Nozzles are located between the settling chamber and the test section, this structure, which has a converging and diverging form, is designed to reach the required Mach number in the test section. The subsonic speed in the rest room reaches the speed of sound due to the expansion after the throat part of the "nozzle". If the required pressure ratio is set, a supersonic nozzle is a convergent–diverging device that allows the flow to transition from subsonic to supersonic flow conditions [8].

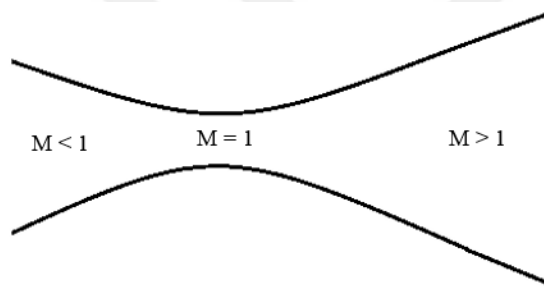


Figure 1.3. Nozzle geometry

One technique for calculating supersonic irrotational flow is the method of characteristics. This method uses a sequence of points distributed along the nozzle for which we know the flow parameters and lines linking these points, known as characteristic lines, to build the divergent portion of the nozzle [9]. Unique forms for the diverging part of the Laval nozzle are needed for each test section Mach number in order to provide a uniform Mach number distribution, which is necessary for wind tunnels [10].

Alongside the more traditional solid wall test sections, supersonic tunnels are sometimes arranged so that testing is done as a fully open or closed free jet without a diffuser. The scaled models are tested under the desired conditions in the test section and the necessary data are obtained.

In wind tunnels, load measurement systems are used to measure the forces and moments that models are generally exposed to in multiple axes (generally 6 components). These loads are generally examined in two parts as static and dynamic loads. Static load

measurement systems are used in most of the wind tunnels because of ease of use and more accurate results. Figure 1.4 shows the forces and moments that act on a model.

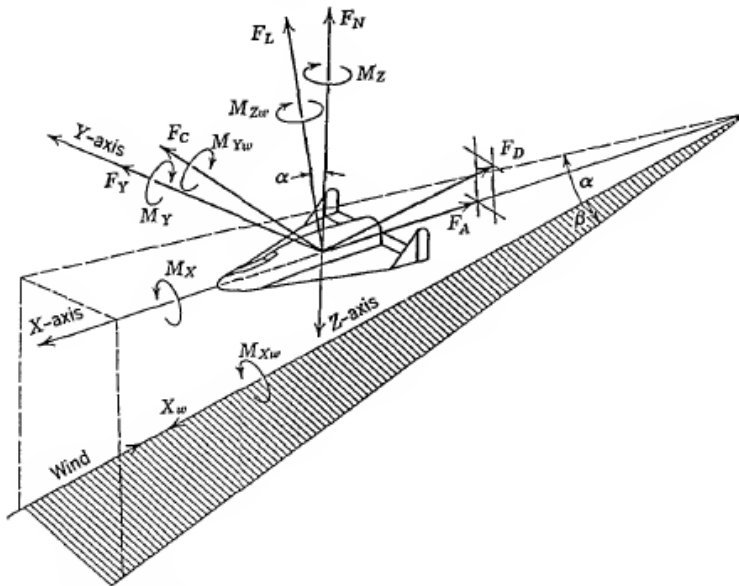


Figure 1.4. Forces and moments acting on the model under test

Most supersonic wind tunnels are built with a diffuser with a convergent section, a zone of minimal cross section called a "second throat", and then a divergent section. The test section Mach number is progressively slowed by a sequence of reflecting oblique shocks produced by the converging geometry, until a weak normal shock at the diffuser's end causes the flow to reach subsonic speed [11, 12].

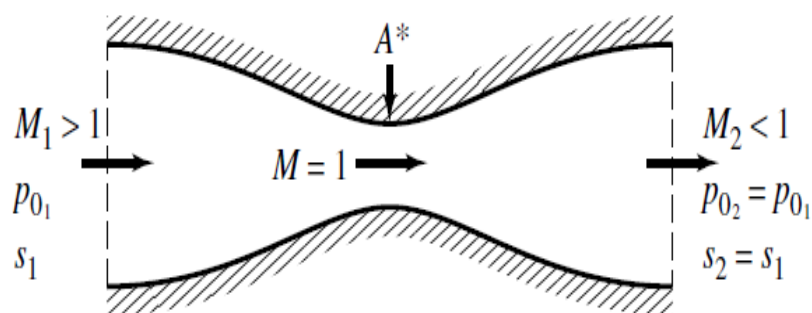


Figure 1.5. General view of diffuser geometry

The noise of a high-speed wind tunnel can be irritating and cause serious health problems at close range. Silencers are designed to reduce the sound of the system.

Within the scope of this study, supersonic wind tunnels are those whose normal operating speeds require the inclusion of compressible flow effects are researched. The flow is assumed as adiabatic that means there is no heat transfer and it is reversible [13]. Assuming isentropic expansion through the nozzle, it is possible to estimate the total operating time of the tunnel during which the supersonic flow fills the diverging section of the nozzle [14]. The test section cross-sectional dimensions are chosen as 0,4 m by 0,4 m and maximum speed is aimed as Mach 4. The type of the tunnel is chosen to be blow-down considering its relatively low cost and capability of operating at different Reynolds numbers. Preliminary calculations are performed to obtain a run time of 60 seconds at the speed of Mach 4, assuming the outlet pressure as atmospheric pressure at sea level.

12 different supersonic and trisonic tunnels are compared with respect to their Mach envelope, Reynolds number, test section dimensions, run time, tank capacity and stagnation pressure. There are some missing informations about several items due to lack of corresponding data in literature. Main objective of this comparison is to validate the goals of our design with current supersonic tunnels around the world.

All the tunnels are chosen as intermittent blow-down type. They differ in their test section size (some of them are very large sized). CAAA and ISL tunnels are most similar tunnels comparing to our design in terms of test section size and Mach envelope. Table 1.1 compares 12 supersonic blowdown wind tunnels to our design in terms of major properties.

Table 1.1. Supersonic & Trisonic wind tunnels

	Tunnel Name	Type of the Tunnel	Test Section Size (in mm.)	Mach Envelope	Reynolds Envelope	Runtime	Tank Capacity / Mass Flow Rate	Stagnation Pressure
1	INCAS (Romania)	Trisonic	1200 x 1200	1.1 - 3.5	100 x 10 ⁶ - 150 x 10 ⁶	5 - 60 sec.	1985 m ³ (three tanks)	
2	ITU Trisonic Wind Tunnel (Turkey)	Trisonic	150 x 150	0.4 – 2.2 & 2.2 – 4.0				

Table 1.1. (continued) Supersonic & Trisonic wind tunnels

3	BAE Supersonic Wind Tunnel (BAE)	Supersonic	1200 x 1200	1.4-3.8		up to 30 sec.		
4	VTI T-38 (Spain)	Trisonic	1500 x 1500	0.2 - 4.0	up to 115 $\times 10^6$			
5	DSTO (Australia)	Transonic	806 x 806	0.3 to 1.2 & 1.4	2×10^6 - 3×10^6			
6	University of Sydney, Supersonic Wind Tunnel (Australia)	Supersonic	200 x 200	1.6 - 3.5		more than 2 min.		
7	Von Karman Institute (Belgium)	Supersonic	800 x 100	3.5	50×10^6	8 - 25 min.		3 - 18 bar
8	CAAA (China)	Supersonic	600 x 600	0.4 - 4.5	12×10^6 -30×10^6			up to 15 atm
9	Flow Science Limited, Goldstein Research Lab. (England)	Transonic / Supersonic	210 x 150	0.3 - 2.0		45 sec.	130 m ³	
10	ISL S-30 (France)	Supersonic	300 x 300	1.5 - 4.4	up to 2×10^6	30 - 120 sec.		1.2 - 20 bar
11	JAXA (Japan)	Supersonic	1000 x 1000	1.4 - 4.0	20×10^6 - 60×10^6	40 sec.	280 kg/s mass flow rate	150 - 1400 kPa
12	TUDELFT ST-15 (Netherlands)	Transonic / Supersonic	150 x 150	0.7 - 3.0		800 sec.		
13	Our Design	Supersonic	400 x 400	4.0	approx. 25×10^6	60 sec.	40 m ³ tank capacity / 27 kg/s mass flow rate	7.2 bar

2. METHODOLOGY

As mentioned earlier, the tunnel is selected as intermittent blow-down due to its several advantages over the continuous type such as ease of installation, lower cost, and shorter setup time. In this type of tunnel, the air does not circulate in the system and is released into the atmosphere from the outlet of the nozzle. Figure 2.2 shows schematic of the main components of a supersonic blow-down wind tunnel.

A flow diagram is given that represents steps of the progress of this study (see Figure 2.1).

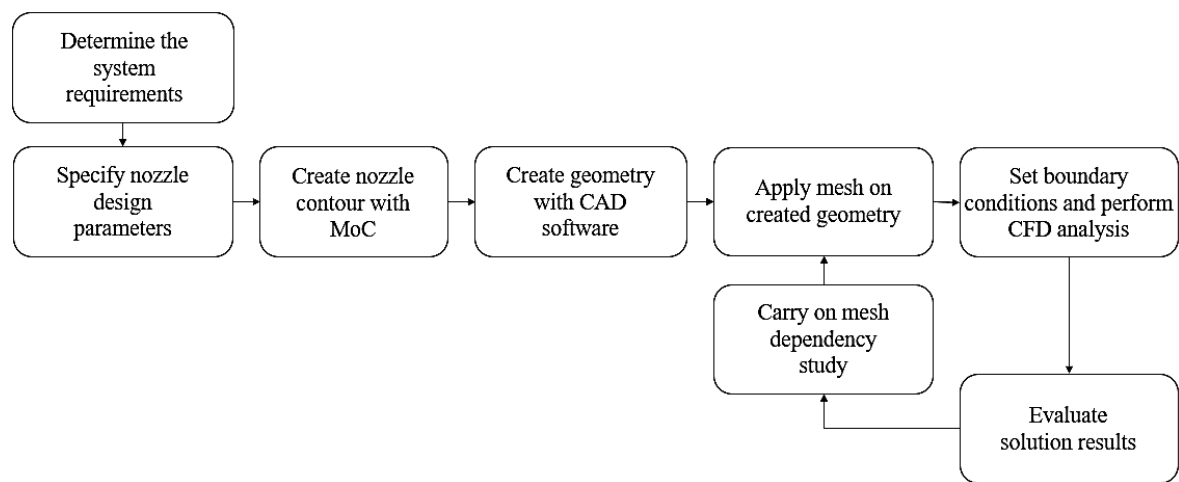


Figure 2.1. Flowchart of the study

The first challenge is to design an appropriate nozzle to have the maximum flow uniformity inside the test section at the desired operating conditions. The second objective is to design a diffuser with minimum losses. For the preliminary design, we assume to have sonic flow at both throats (nozzle and diffuser) as well as isentropic flow through the nozzle. Moreover, the flow is assumed to be adiabatic inside the tunnel. Using these assumptions and the following equations the nozzle and the diffuser throat areas are calculated.

$$A_{t1} \cdot \rho_1^* \cdot a_1^* = A_{t2} \cdot \rho_2^* \cdot a_2^* \quad (2.1)$$

$$A_{t2}/A_{t1} = \rho_1^* \cdot a_1^* / \rho_2^* \cdot a_2^* \quad (2.2)$$

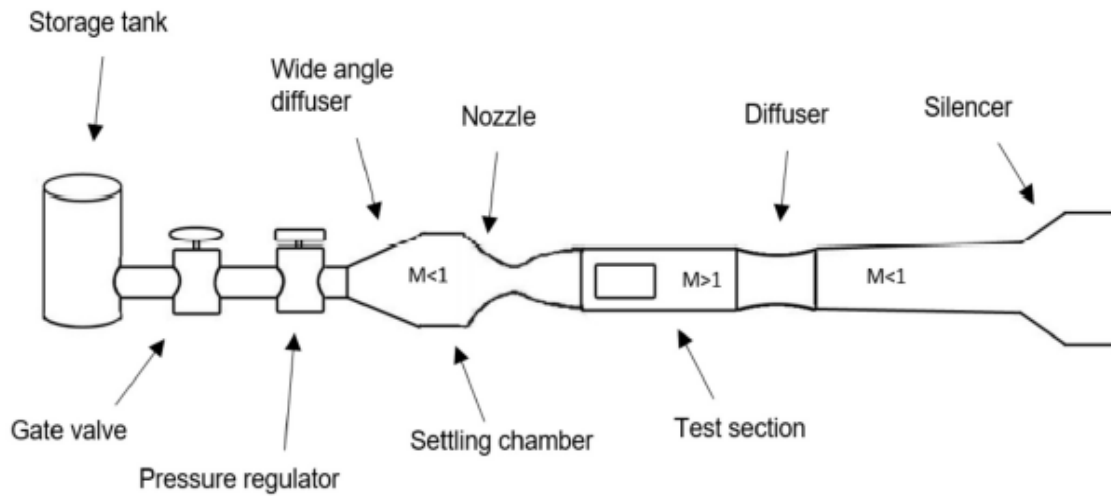


Figure 2.2. Schematic of the main components of a supersonic blow-down wind tunnel

In Eq. 2.1 and Eq. 2.2, A_{t1} and A_{t2} represent the cross-sectional areas of nozzle and diffuser parts, respectively. a_1^* and a_2^* indicate the speed of sound in these parts and are considered to be equal.

$$A_{t2}/A_{t1} = \rho_1^* / \rho_2^* = (P_1^* / RT_1^*) / (P_2^* / RT_2^*) \quad (2.3)$$

Nozzle throat area, A_{t1} , is calculated as $0,015 \text{ m}^2$ by using isentropic flow properties. Also, process is assumed as adiabatic. So, the diffuser cross-sectional area is determined by Equation (2.4):

$$\frac{A_{t2}}{A_{t1}} = \frac{P_1^*}{P_2^*} \quad (2.4)$$

where $T_1^* = T_2^*$ and $A_{t2} = 0,108 \text{ m}^2$

$$P^* = P_0 \left(\frac{2}{\gamma+1} \right)^{\frac{\gamma}{\gamma-1}} \quad (2.5)$$

$$A_{t2} = A_{t1} \times \frac{P_{01}}{P_{02}} \quad (2.6)$$

The pressure ratios $\frac{P_{01}}{P_{02}}$ are estimated as 7,2 from the isentropic flow assumption to achieve Mach 4 at the test section. Required pressure ratio to start the tunnel can be considered as the double of pressure ratio for operating conditions [1, 3].

The mass flow rate at Mach 4 is calculated as 27 kg/s using the following equation:

$$\dot{m} = [A^* \cdot P_0 / \sqrt{T_0}] \cdot \sqrt{\frac{\gamma}{R} \cdot \left[\frac{2}{\gamma+1}\right]^{\frac{\gamma+1}{\gamma-1}}} \quad (2.7)$$

where $A^* = A_{t1}$.

The total mass of the air needed for a 60 seconds tunnel operation is calculated as 1650 kg. Utilizing a compressor with a compression capacity of 40 bars, a reservoir tank of 40 m^3 will be sufficient to store enough air to run the tunnel for 60 seconds.

With the same pressurized air reservoir capacity, if the desired speed in the test section is changed, the operation time changes as well. Table 2.1 and Figure 2.2 shows the run times of the tunnel at different Mach Numbers, beginning from Mach 1,5 up to Mach 4 with 0,5 increment. Our calculations show that the tunnel will have a run time of 111 seconds at Mach 1,5. Tunnel operating pressures which are given in the following table, satisfy the reference values given in Figure 2.2 [3].

Table 2.1. Run times vs. Mach number

Mach Number	Operational Pressure (bar)	Run Time (sec)
1,5	1,08	111
2	1,4	92
2,5	2	81
3	3,04	73
3,5	4,7	67
4	7,2	60

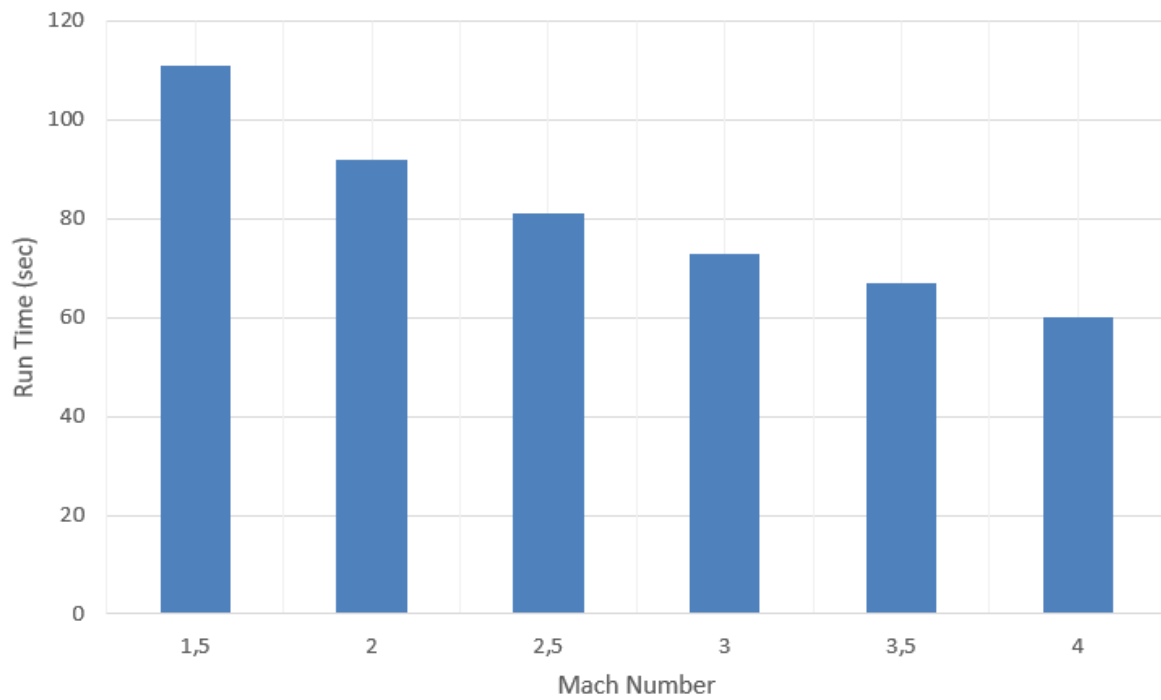


Figure 2.3. Run time vs Mach number

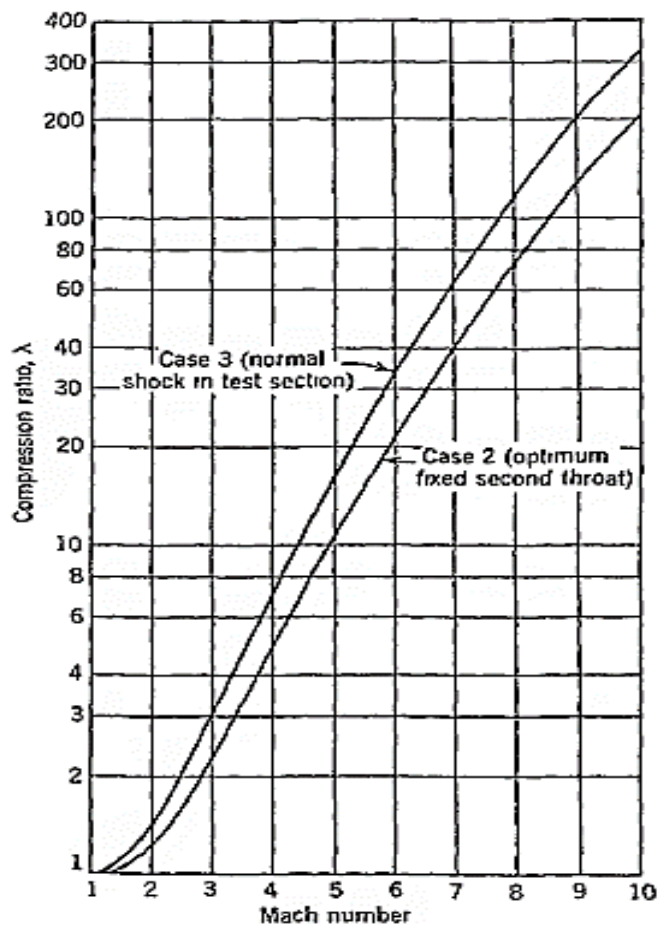


Figure 2.4. Mach Number vs. tunnel compression ratio [3]

2.1. Nozzle Design

The nozzle is most critical part of a supersonic wind tunnel, channeling flow to the test area and accelerating it to a specified speed and condition. Nozzles are not just for wind tunnels; they're also widely utilized in jet engines for propulsion applications.

The supersonic nozzle is made up of two parts: a subsonic component that accelerates the settling chamber flow to sonic speed, and a supersonic segment that accelerates the flow even further and delivers it to the test section as a uniform stream [3].

Achieving the desired and appropriate velocity in the wind tunnel is highly dependent on the nozzle contour properties, with the definition of the nozzle contour being a function of both the aerodynamic and physical properties of the nozzle design [15]. In a convergent divergent nozzle, the reduction of the flow cross section in the case of a subsonic flow leads to acceleration of the gas. The flow surface converges until the minimum surface area, that is the throat. In the throat, the current flows at the speed of sound. Downstream of the geometry, the diverging section can accelerate the gas to the supersonic limit [16].

There are two main categories of supersonic nozzles: minimum length nozzles and gradually expanded nozzles. Minimum length nozzles are commonly used to decrease the weight and length of the nozzle, especially in rockets and jet engines. They are especially used for an optimization of nozzle thrust efficiency is an important factor [17]. Gradual-expansion type nozzles are generally used where providing a high-quality flow is a significant factor, such as wind tunnels [18].

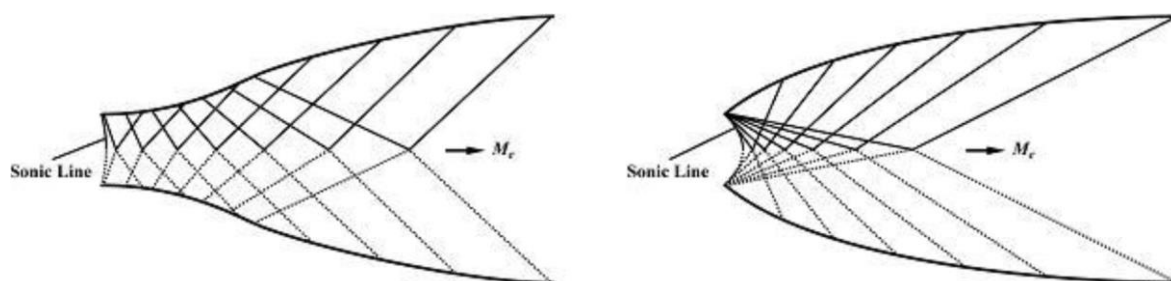


Figure 2.5. Gradual-expansion nozzle (left) vs minimum length nozzle (right)

2.1.1. The Method of Characteristics

The method of characteristic is the most often used direct design methodology for developing the nozzle contour among those used to produce nozzle geometry. Ludwig Prandtl and Adolf Busemann proposed the method of characteristic, which is a graphical approach to solving a flow field, in 1929 [19 - 21]. Method of Characteristics (MoC) is a suitable numerical method for solving two-dimensional compressible flow problems. Using this technique, flow characteristics such as direction and velocity can be calculated at different points throughout the flow field [3, 11].

For both two-dimensional and three-dimensional flows, the method of characteristics was devised. However, the two-dimensional flow technique is commonly used due to its ease of application. A rectangular supersonic nozzle with parallel side walls and curved top and bottom walls is an example of a two-dimensional flow with flow changes in two dimensions.

The idea behind the Characteristics Method (MoC) in terms of nozzle design is the expansion of the steady supersonic flow through the use of expansion waves. The opposite of shock compression waves, which impede airflow, are these Mach waves [22]. This is governed by the Prandtl-Meyer function:

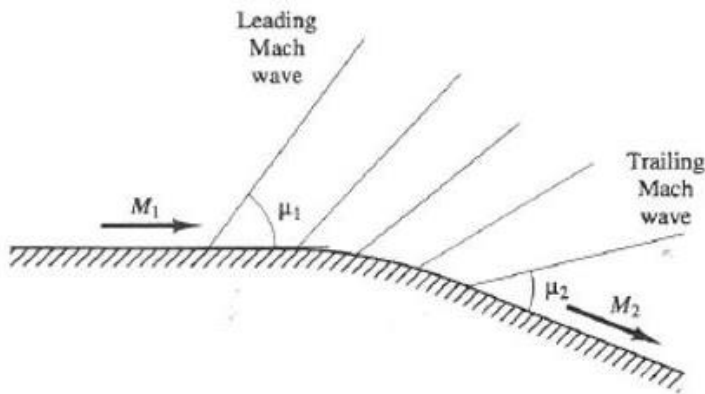


Figure 2.1.1. Gradual expansion of supersonic flow [22]

$$dv \pm d\theta = \sigma \frac{\sin \theta \sin \mu}{y} ds \quad (2.8)$$

$$v = \sqrt{\frac{\gamma+1}{\gamma-1}} \arctan \sqrt{\frac{\gamma+1}{\gamma-1} (M^2 - 1)} - \arctan \sqrt{M^2 - 1} \quad (2.9)$$

The parameter ν is known as the Prandtl-Meyer angle and where Mach angle, μ , is defined as [21]:

$$\mu = \sin^{-1} \frac{1}{M} \quad (2.10)$$

The parameters are as follows: θ is the flow angle with respect to the nozzle centerline, s is the arc length along the characteristic, y is the radial distance, γ is the specific heat ratio, and μ is the Mach angle, which is defined as $\arcsin(1/M)$. In the case of axisymmetric flow, $\sigma = 1$, and for 2-D flow, $\sigma = 0$. Radian is used for all angles. The "+" in Equation (2.8) denotes right-running traits as well as the "-" to left-running traits. Mach lines are angles that radiate from a point. $\theta + \mu$ represents the left characteristic and $\theta - \mu$ represents the right characteristic. Equation (2.8) is used to calculate the Mach lines defined by:

$$\frac{dy}{dx} = \tan(\theta \pm \mu) \quad (2.11)$$

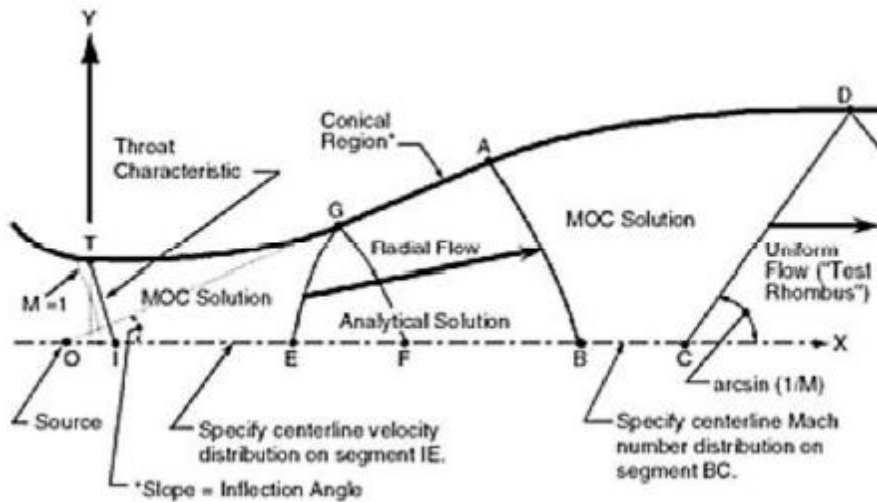


Figure 2.1.2. Design procedure of nozzle geometry [23]

A MATLAB code is utilized to perform the method of characteristic. 100 characteristic lines were created with this program to solve nozzle geometry. As the number of lines increases, created nozzle wall contour gets smoother. However, over 100 characteristic lines, there was no improvement on the boundary and also some conflicts occurred. Figure 2.7 and 2.8 show the 2 Mach and 4 Mach nozzle contours, results of MoC. Outputs of the MATLAB code are also obtained as x and y-axis coordinates. To create the geometry of the nozzle, these coordinates are imported to a computer-aided drawing program. Figure

2.9 and Figure 2.10 shows the created nozzle geometry. Area ratio between outlet of the nozzle and the throat is found as 10,72 which is consistent with previous calculations assuming isentropic flow condition through the nozzle.

That geometry, which created by using MATLAB, creates a boundary beginning from the throat ends with the exit of the nozzle i.e. entrance of the test section. Nozzle exit is extended for half length of the test section where the model will be placed [3]. To create inlet geometry of the nozzle, hyperbolic tangent function was used. The hyperbolic tangent function, often denoted as \tanh , is a mathematical function commonly used in various fields, including mathematics, physics, and machine learning. It is widely used in neural networks and other mathematical models due to its desirable properties, such as being differentiable and mapping input values to a bounded range.

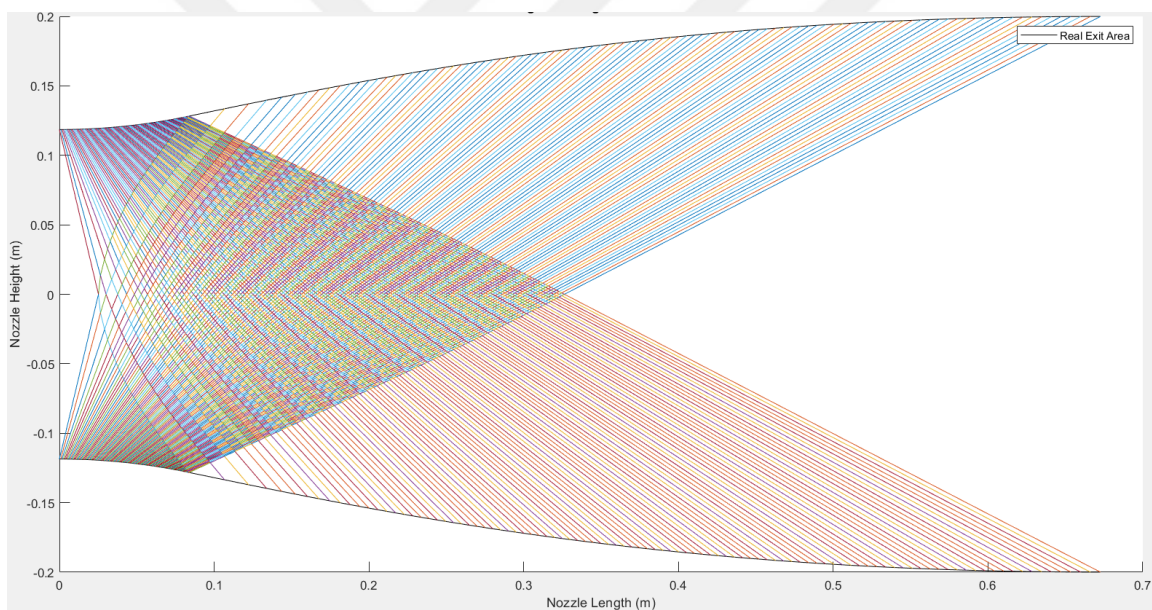


Figure 2.1.3. Mach 2 nozzle contour

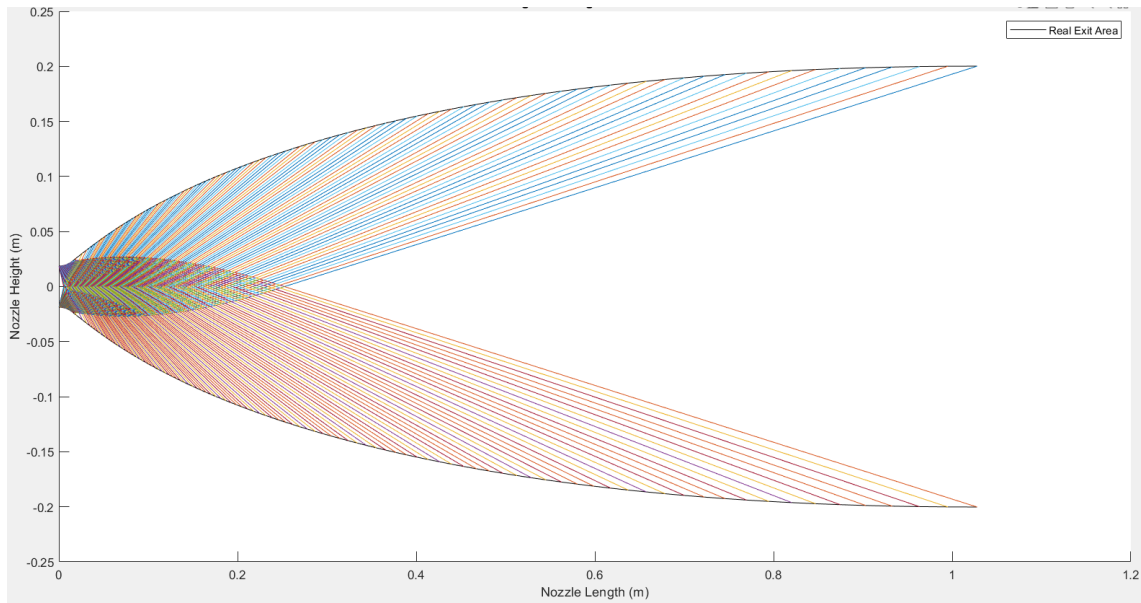


Figure 2.1.4. Mach 4 nozzle contour

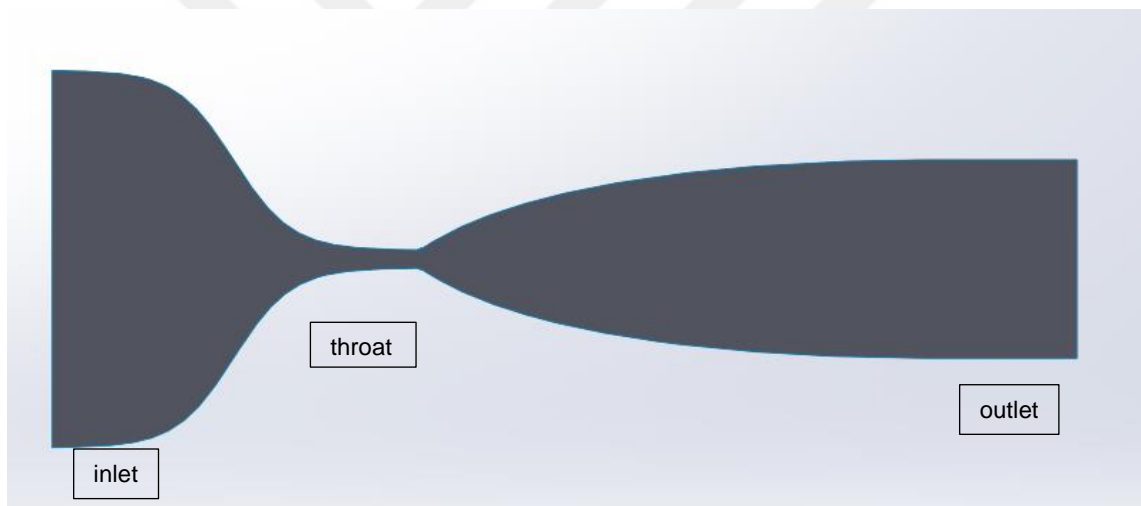


Figure 2.1.5. Mach 4 nozzle geometry

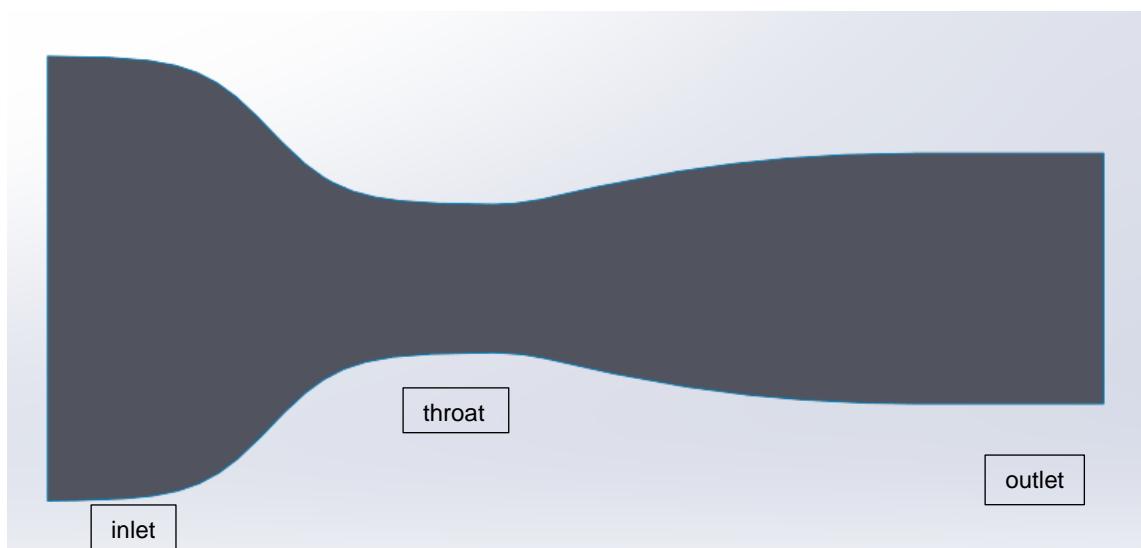


Figure 2.1.6. Mach 2 nozzle geometry

2.2. CFD Analysis

Besides the wind tunnel testing, Computational Fluid Dynamics (CFD) analysis has an important role on design and development of aerial vehicles. CFD methods are used to simulate the real flight conditions of an aircraft. Both wind tunnel testing and CFD are performed to estimate the behavior of a model that is flying through the air. Great fidelity of CFD approaches improves wind tunnel testing [24, 25].

The flow quality of the wind tunnel test section is related to the temporal and spatial aspects of the flow. Along the streamwise tunnel axis, distributions of flow specify the flow quality [26]. The flow evolution and its quality can be checked by using CFD (Computational Fluid Dynamics) analysis. ANSYS Fluent 2023 R1 provides comprehensive modeling capabilities for various laminar and turbulent compressible and incompressible fluid flow problems. For all flows, ANSYS Fluent 2023 R1 solves mass and moment conservation equations. Additionally, for flows involving heat transfer or compressibility, it also considers energy conservation equation [14].

There are two main solver types as pressure-based and density-based in Fluent. For highspeed flows, a density-based solver is a better option due to high compressibility of the air in supersonic flows. The density-based solver simultaneously solves the equations that govern continuity, momentum, and (when appropriate) the transfer of energy and species [14].

Despite that the flow can be assumed inviscid in supersonic conditions, an inviscid CFD analysis is not suitable to investigate the boundary layer development. So, a different turbulence model must be used.

To perform the simulation, $k - \omega$ SST (shear stress transport) turbulence model is utilized. This model is widely used in many aerodynamic applications involving boundary layer evolution. Basically $k - \omega$ SST combines two equations $k - \omega$ on near the wall and $k - \epsilon$ model in the free-stream. It gives a better solution compared to the inviscid model and other viscous models on boundary layer.

3. CFD SIMULATIONS RESULTS AND DISCUSSION

CFD analysis of the nozzle of the designed supersonic wind tunnel will be presented in this section. Firstly, designed geometry is meshed by using Fluent Meshing and Pointwise softwares. For this process Y^+ value (will be discussed in following sections) is estimated. Then providing the mesh quality criteria, different sized meshes are applied on the geometry for both 2D and 3D models. CFD analysis are performed based on these references and considering the computational limits of existing hardware (work station computer).

3.1. Y^+ Estimation

When constructing the mesh, it is often useful to be able to estimate the wall-distance needed to obtain a certain Y^+ value. To estimate this, the following steps can be applied:

1. Compute the Re number:

$$Re = \frac{\rho \cdot U_{freestream} \cdot L_{boundary\ layer}}{\mu} \quad (3.1)$$

2. Estimate the skin friction

$$C_f = [2 \cdot \log_{10}(Re_x) - 0,65]^{-2,3} \text{ for } Re < 10^9 \quad (3.2)$$

3. Compute the Wall shear stress:

$$\tau_w = C_f \cdot \frac{1}{2} \cdot \rho \cdot U_{freestream}^2 \quad (3.3)$$

4. Compute the Friction velocity:

$$u_* = \sqrt{\frac{\tau_w}{\rho}} \quad (3.4)$$

5. Compute the wall distance:

$$h = \frac{y^+ \cdot \mu}{\rho \cdot u_*} \quad (3.5)$$

Where ρ is density u_* is friction velocity, h is first layer thickness and μ is dynamic viscosity.

Y^+ value should be in the range 1-30. As the Y^+ value decreases, the mesh quality increases. Considering the capacity of the computers, that value is selected average of the

limits, as 15 for 3D CFD analysis and 1 for 2D CFD analysis. So, the first layer thickness is calculated by using Equation (3.1) – Equation (3.5).

To estimate the first layer thickness, following inputs given in Table 3.1.1 and Table 3.1.2 were used:

Table 3.1.1. Y+ Calculation inputs for Mach 4

Input	Value
Freestream velocity	4 Mach $\sim 1384 \frac{m}{s}$
Freestream air density	$0,0577 \frac{kg}{m^3}$
Boundary layer length	1300 mm
Desired Y+ value	1 (for 2D analysis) – 15 (for 3-D analysis)

Table 3.1.2. Y+ Calculation inputs for Mach 2

Input	Value
Freestream velocity	2 Mach $\sim 692 \frac{m}{s}$
Air density	$0,220 \frac{kg}{m^3}$
Boundary layer length	1000 mm
Desired Y+ value	1 (for 2D analysis) – 15 (for 3-D analysis)

Air density and dynamic viscosity values were obtained by using ideal gas properties at desired velocity and pressure inside the test section at the altitude of the facility ($\sim 1200m$). The boundary layer lengths were measured from the created geometry on Solidworks.

Providing the desired Y+ value, different sized meshes are applied on the geometry. Following criteria were utilized to improve the mesh quality [14]:

- Orthogonal Quality in meshing refers to the degree to which the angles between neighboring elements (such as triangles or quadrilaterals in 2D, or tetrahedra or hexahedra in 3D) are close to being perfectly perpendicular (90 degrees). A mesh with higher orthogonal quality has elements that approach a state of orthogonality, meaning the angles between them are closer to 90 degrees.

- Skewness is the measure of how much the shape of a cell differs from that of an equilateral cell with the same volume.
- Aspect Ratio in meshing refers to the ratio of the longest side of an element (such as a triangle or quadrilateral in 2D, or a tetrahedron or hexahedron in 3D) to its shortest side. In simpler terms, it measures the elongation or distortion of an element's shape. A low aspect ratio indicates that the element is closer to being equilateral or cube-shaped, while a high aspect ratio suggests that the element is stretched or distorted (must be lower than 20-30) [14].

Mathematically, the aspect ratio (AR) of an element can be defined as:

$$AR = \frac{\text{Longest side length}}{\text{Shortest side length}}$$

3.2. Mesh Dependency

A mesh dependency study is a process used in numerical simulations, particularly in the context of finite element analysis (FEA) or computational fluid dynamics (CFD). In numerical simulations, the computational domain is discretized into smaller elements or cells, forming a mesh. The accuracy of the simulation results is influenced by the quality and density of this mesh.

The purpose of a mesh dependency study is to assess how sensitive the simulation results are to changes in the mesh size or refinement. This involves running the simulation with different mesh resolutions and analyzing how the results change as the mesh is refined or coarsened.

Another goal of a mesh dependency study is to ensure that the simulation results are not excessively influenced by the choice of mesh and that the results are reliable and accurate. It helps in optimizing the computational resources by using a mesh that is fine enough to capture important features of the problem without unnecessary computational cost.

3.3. Boundary Conditions & Initial Conditions

To perform CFD analysis Fluent needs boundary and initial conditions as input values. In this setup, density-based solver is chosen as it has a better accuracy than pressure-based

solver for compressible flows. For Mach 4 geometry, inlet and outlet conditions are selected as pressure-inlet and pressure-outlet and their values are 7,2 bar and 4611 pascal, respectively from the calculations mentioned before. By using the same calculations, Mach 2 boundary conditions were found as 1,4 bar and 17894 pascal, respectively. The no-slip condition is enforced at the boundaries of the surface, resulting in a velocity of zero at the wall. This is a common characteristic of viscous flow within the boundary layer. For initial conditions of the environment standard room conditions are chosen. To provide compressibility effect on air, ideal gas properties are used.

3.4. 2D CFD Analysis

Considering the mesh quality criteria and desired Y^+ value, $5,6 \times 10^{-6} m$ of first layer thickness is calculated for Mach 4 nozzle geometry and $3,14 \times 10^{-6} m$ for Mach 2 nozzle geometry. Achieving square-shaped meshes at the middle of the geometry, growth rate and number of layers - given in Table 3.4.1 and Table 3.4.2 - were obtained.

Table 3.4.1. Mesh dependency study of 2D model for Mach 4

Mesh Number (million)	First Layer Thickness (m)	Growth Rate	Orthogonal Quality	Y^+ Value
1	$1,33 \times 10^{-3}$	1,2	>0,71	~12,3
2	$6,66 \times 10^{-4}$	1,15	>0,72	~9,82
4	$3,33 \times 10^{-5}$	1,12	>0,72	2,8
8	$5,6 \times 10^{-6}$	1,019	>0,72	~1,21

Table 3.4.2. Mesh dependency study of 2D model for Mach 2

Mesh Number (million)	First Layer Thickness (m)	Growth Rate	Orthogonal Quality	Y^+ Value
1	$1,00 \times 10^{-4}$	1,15	>0,71	~11,39
2	$3,00 \times 10^{-5}$	1,12	>0,72	~3,435
4	$1,00 \times 10^{-5}$	1,1	>0,72	1,126
8	$3,14 \times 10^{-6}$	1,015	>0,72	~0,79

Growth rate is generally chosen between 1-1.2. As this value decreases, accuracy of the solution increases. So, for this study it is chosen lower rates to get better results.

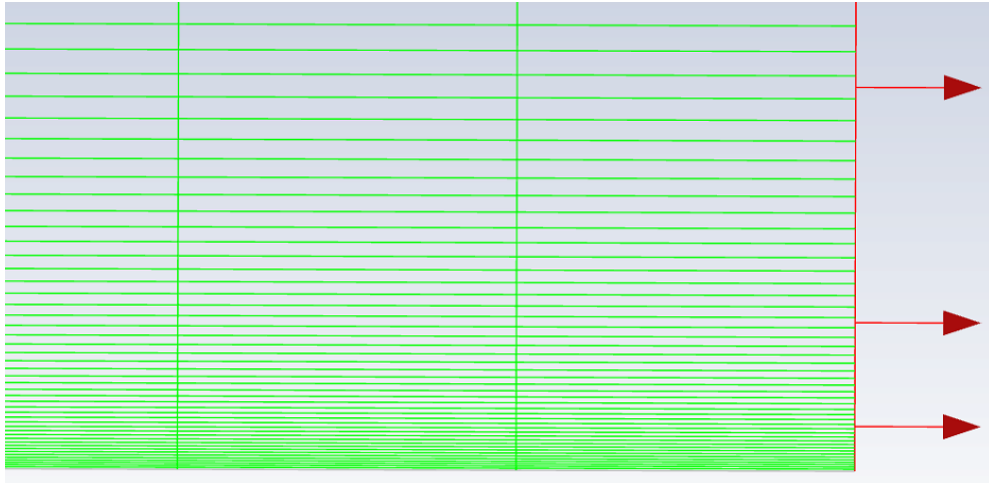


Figure 3.4.1. Close view of surface mesh

After the meshing process is done, ANSYS Fluent 2023 R1 software is used to perform CFD analysis on 2D model for both 2 geometries. As can be seen in Figure 3.4.2 to Figure 3.4.5, the airflow inside the test section can reach the desired Mach numbers. Also, results of the solution at the boundary are satisfactory. Figure 3.4.8 to 3.4.10 shows the Mach number vertical distribution at the outlet of the nozzle between solutions in terms of mesh number. Also, mesh convergence study is performed. Ensuring that the model has reached a solution is confirmed by a mesh convergence investigation (see Figure 3.4.11 to Figure 3.4.14). Further refining is not required because it also offers support for mesh independence. Nozzle walls surface pressure distributions are shown in Figure 3.4.6 and Figure 3.4.7.

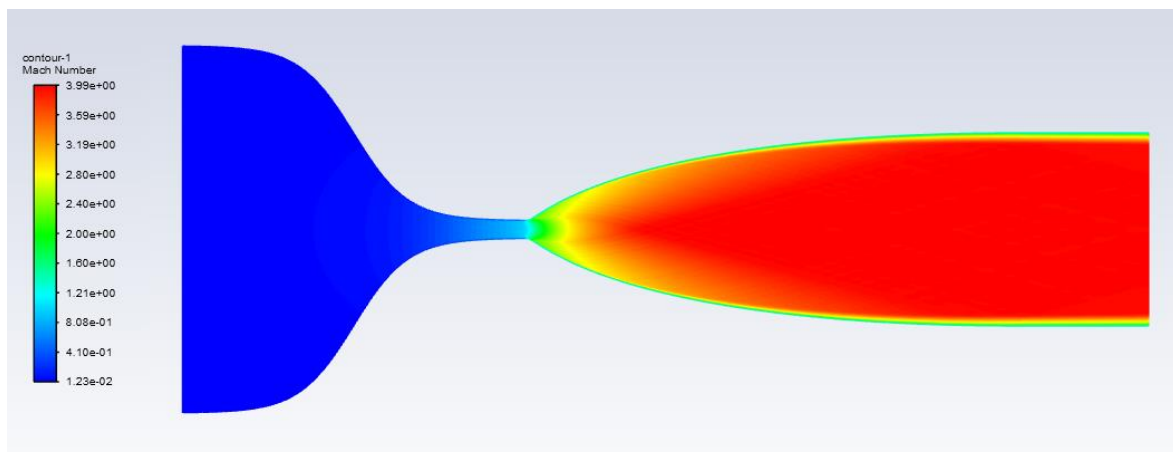


Figure 3.4.2. Mach number contour from the Fluent simulation of the Mach 4 nozzle geometry

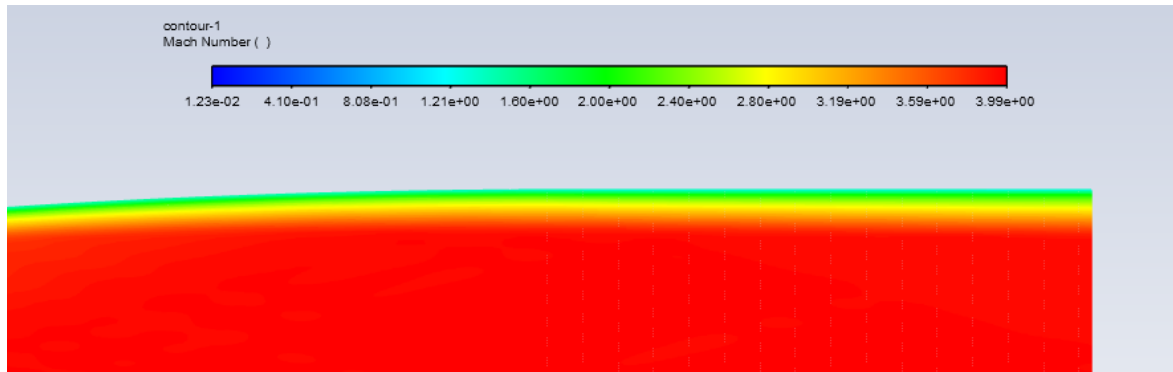


Figure 3.4.3. Mach 4 geometry velocity contour of the boundary layer

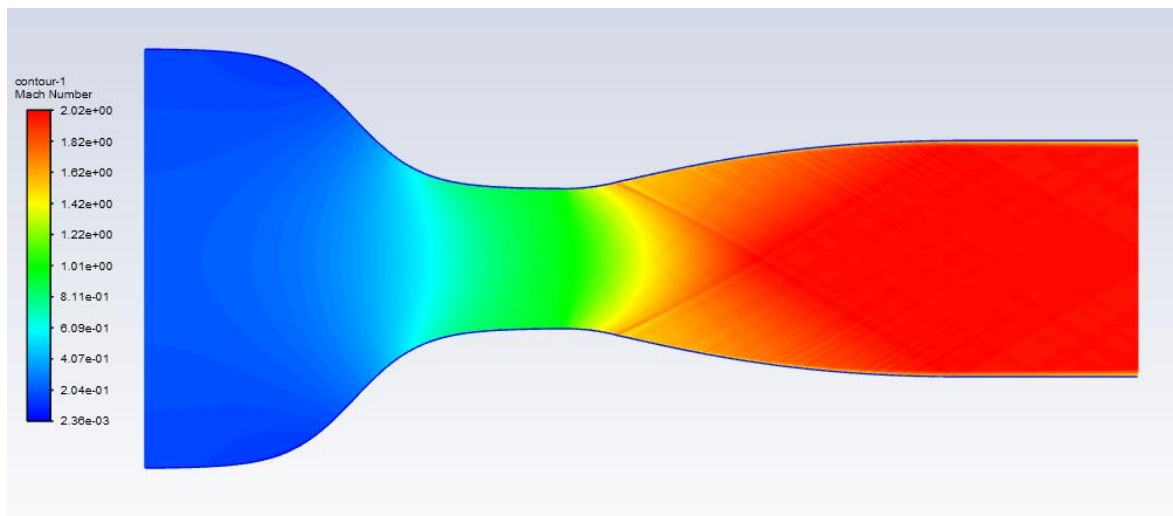


Figure 3.4.4. Mach number contour from the Fluent simulation of the Mach 2 nozzle geometry

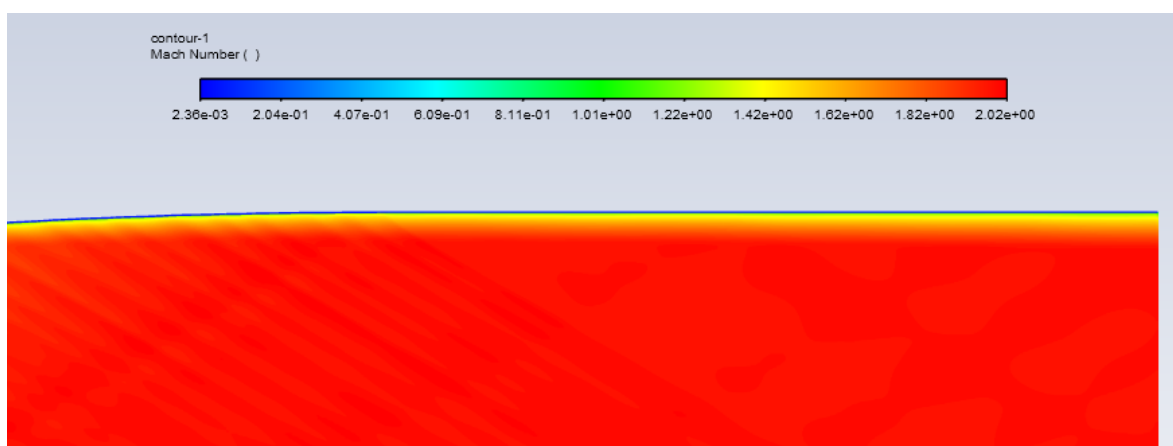


Figure 3.4.5. Mach 2 geometry velocity contour of the boundary layer

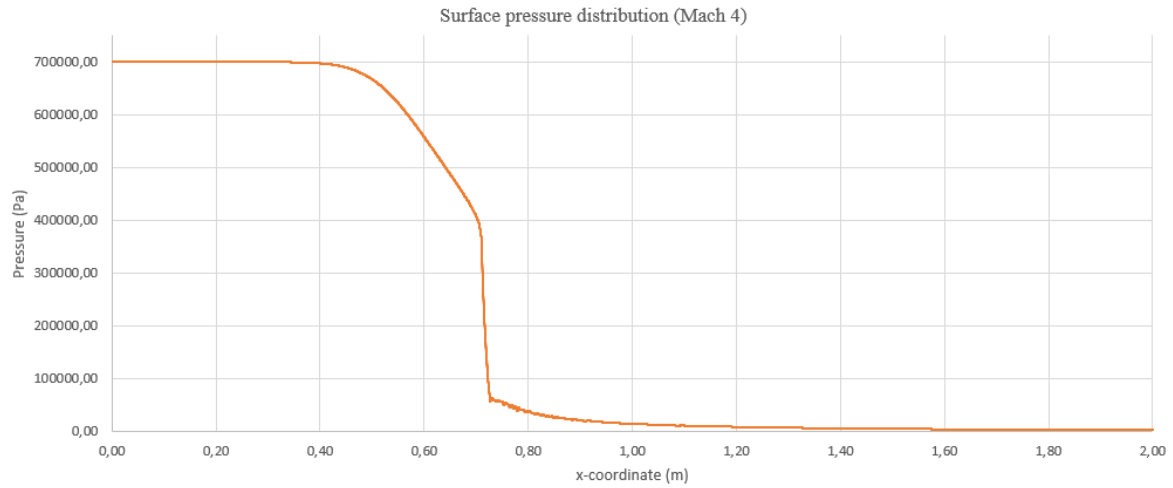


Figure 3.4.6. Surface pressure distribution for Mach 4 nozzle

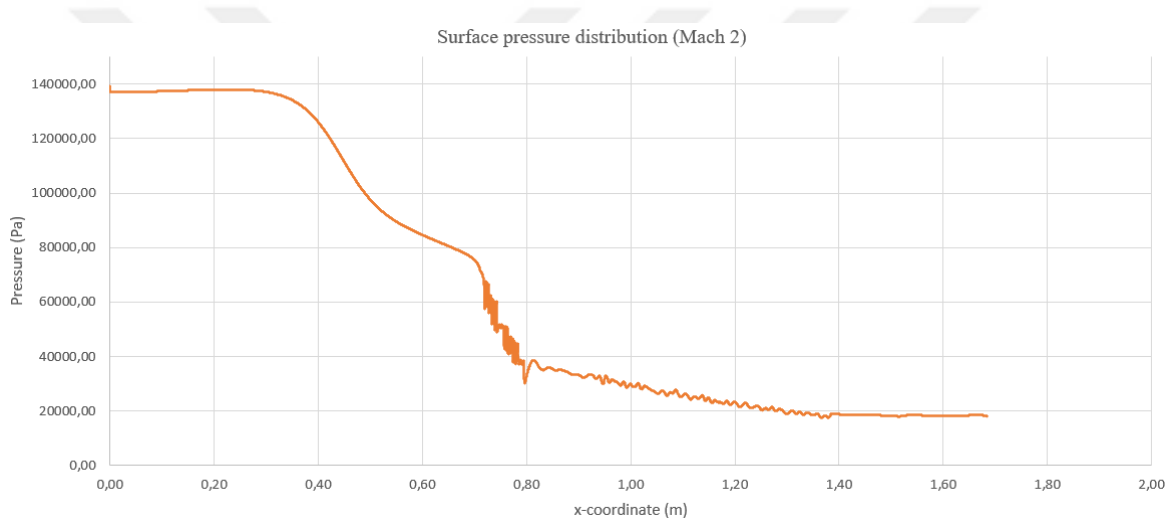


Figure 3.4.7. Surface pressure distribution for Mach 2 nozzle

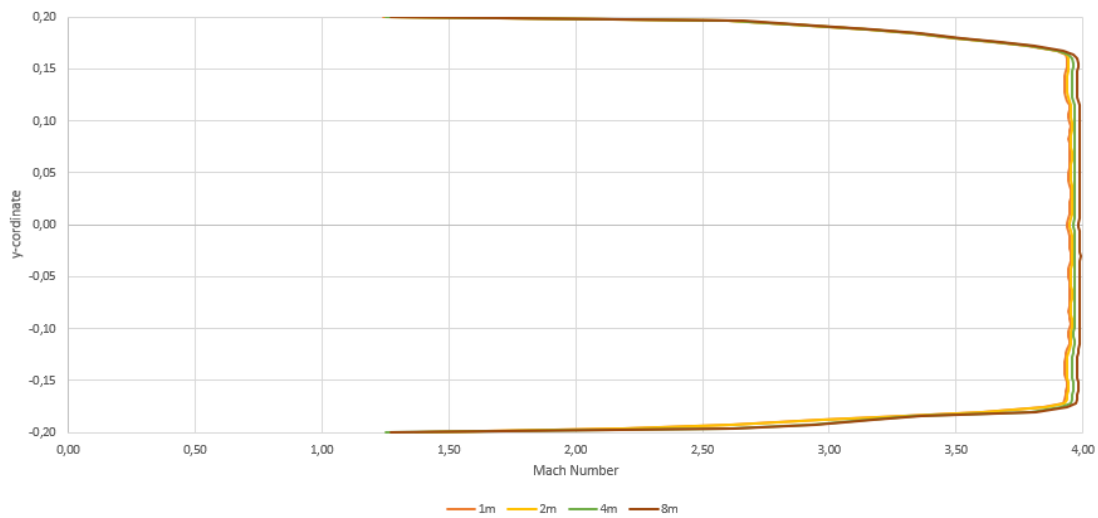


Figure 3.4.8. Mach number vertical distribution in the outlet of the nozzle for different mesh numbers (in millions) (Mach 4)

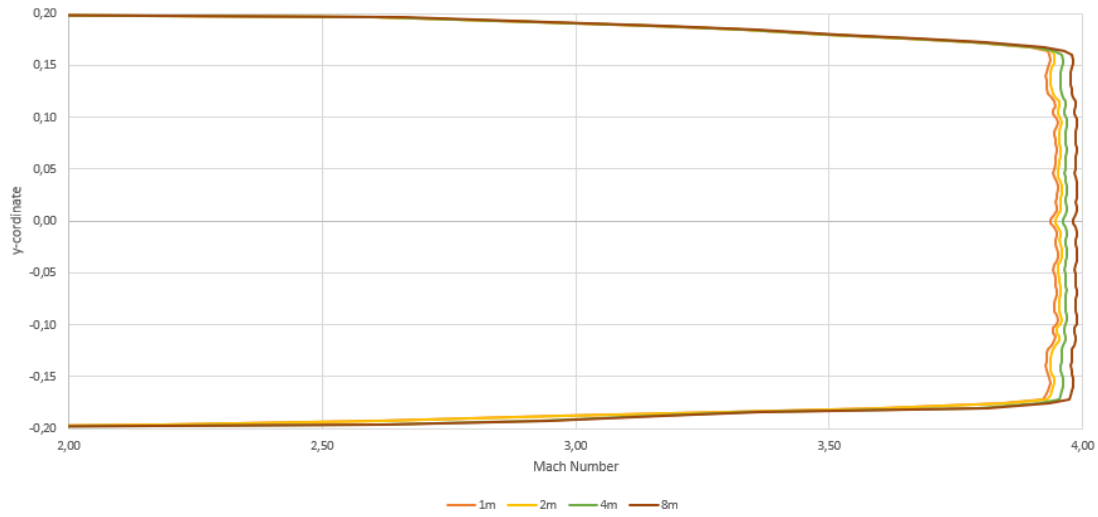


Figure 3.4.9. Mach number vertical distribution in the outlet of the nozzle for different mesh numbers (in millions) in a close range (Mach 4)

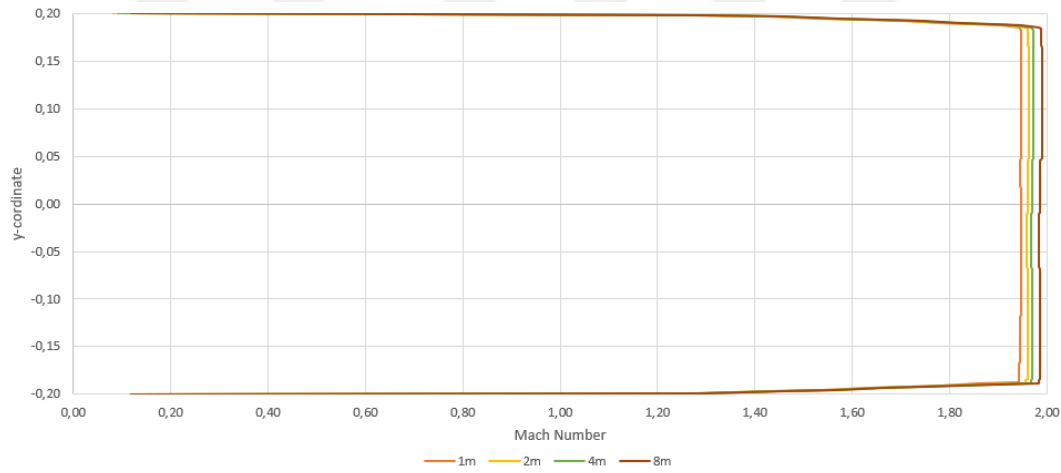


Figure 3.4.10. Mach number vertical distribution in the outlet of the nozzle for different mesh numbers (in millions) in a close range for Mach 2

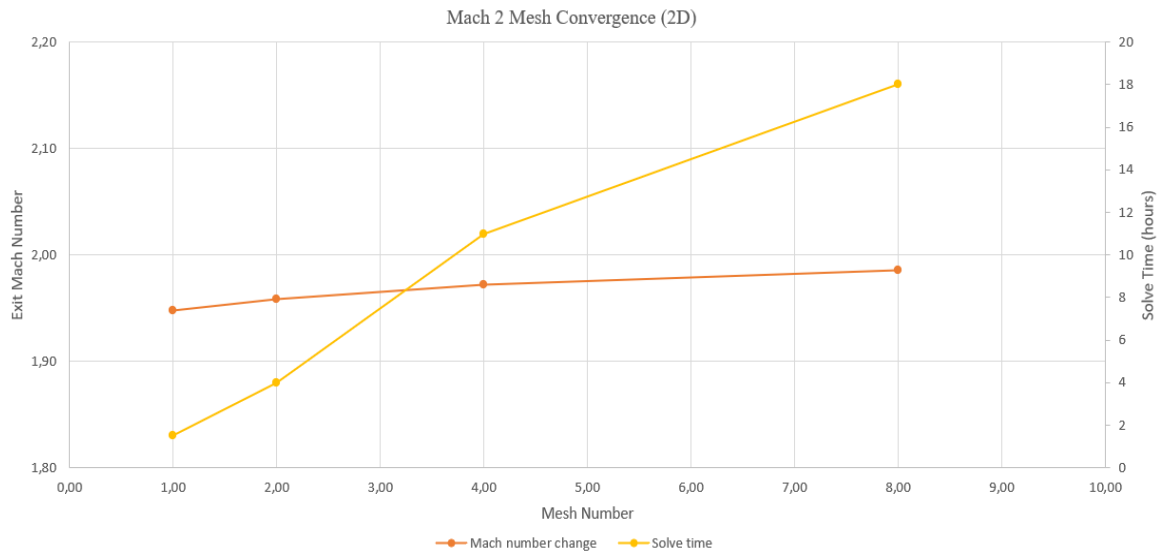


Figure 3.4.11. Mach 2 nozzle mesh convergence study (2d)

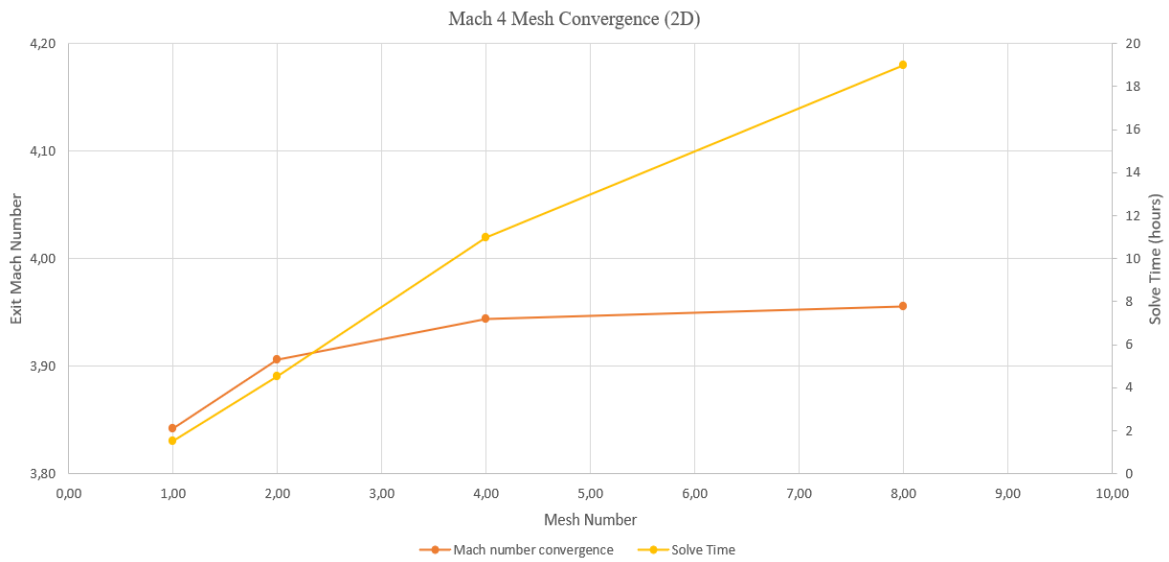


Figure 3.4.12. Mach 4 nozzle mesh convergence study (2d)

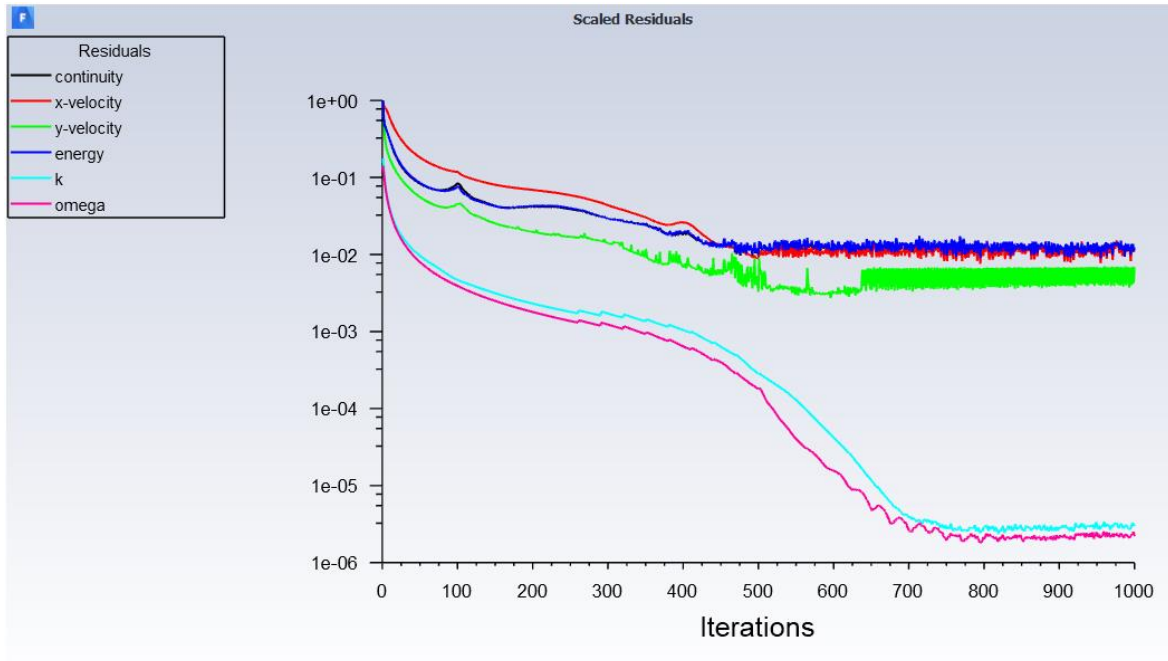


Figure 3.4.13. Mach 2 nozzle mesh convergence plot (2d – 4m mesh)

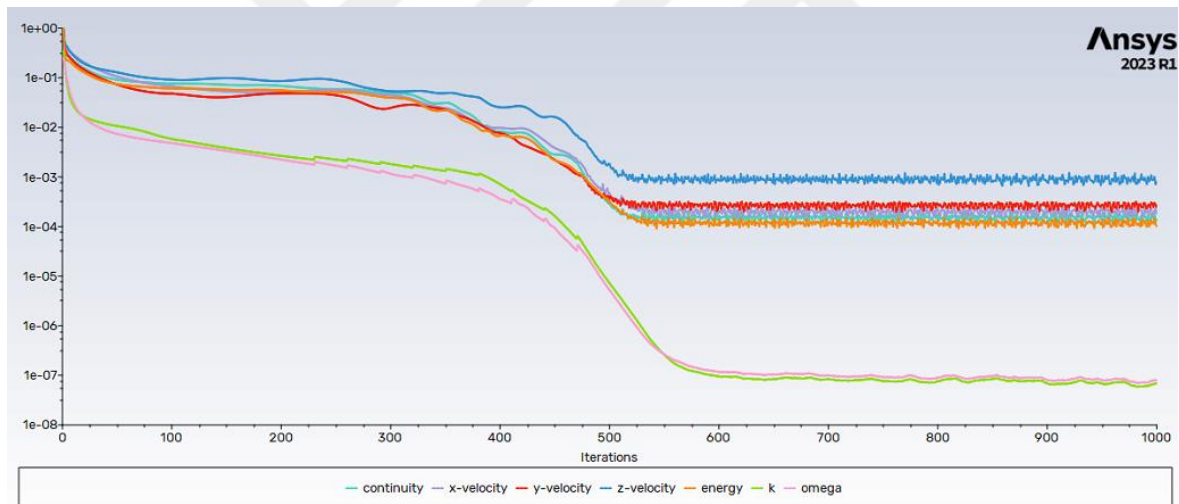


Figure 3.4.14. Mach 4 nozzle mesh convergence plot (2d – 4m mesh)

3.5. Mesh Dependency on Boundary Layer

Mesh dependency study was performed on boundary layer for 2D CFD analysis worked before. Results for different number of meshes (1m, 2.5m, 4m and 5m) were illustrated in Figure 3.5.1 and Figure 3.5.2.

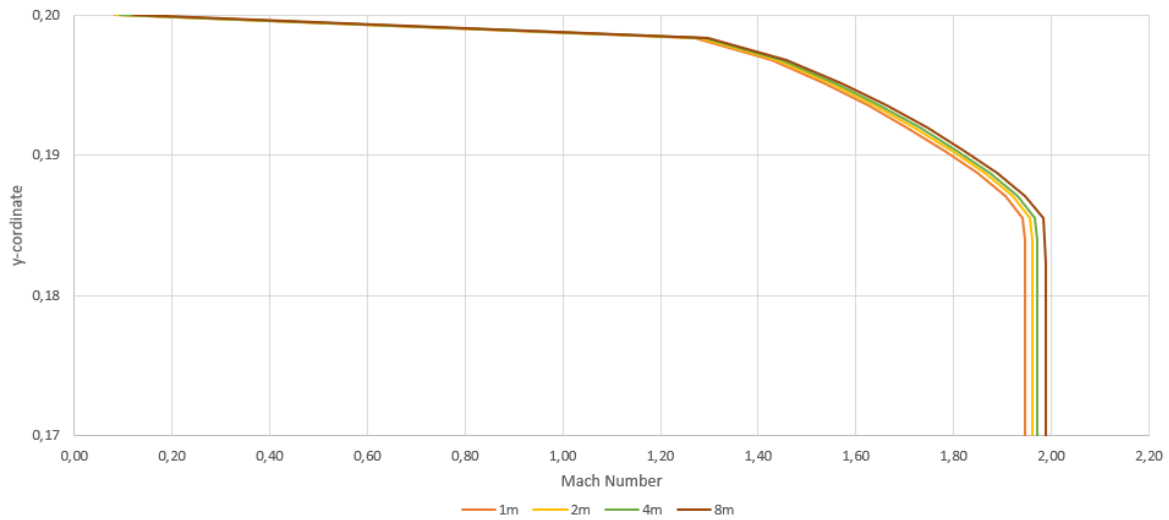


Figure 3.5.1: Mach number distribution at the boundary layer for different Mesh numbers (in millions) (Mach 2)

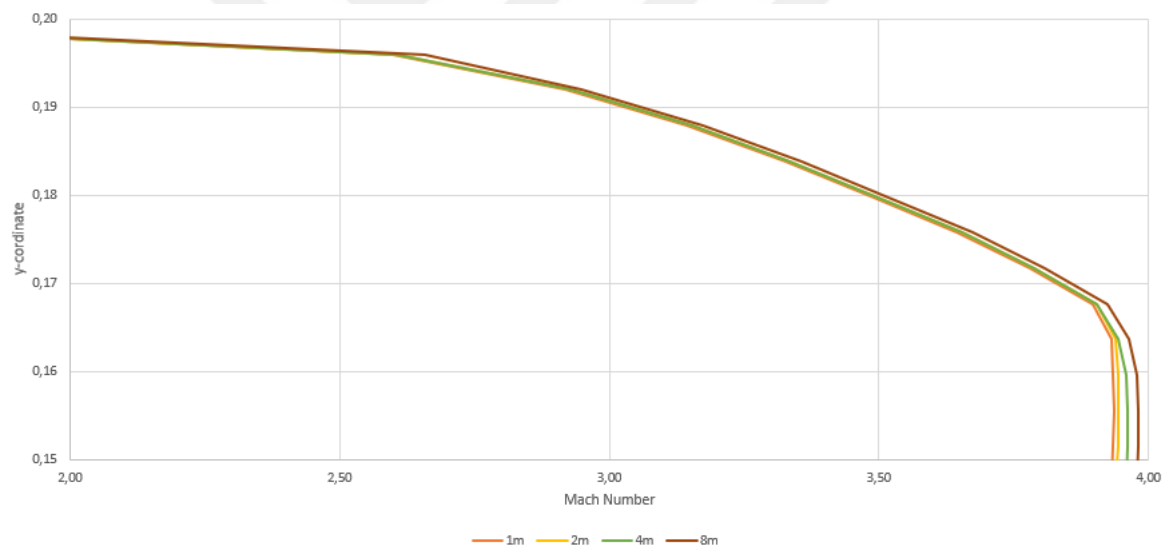


Figure 3.5.2: Mach number distribution at the boundary layer for different mesh numbers (in millions) (Mach 4)

Airspeed in the test section gets uniform approaching to the mid-plane between +0.15 and -0.15 meters. So that the remaining area creates the boundary layer velocity profile given above. Concluding the results, increasing mesh number -with increasing mesh quality- gives better velocity profile solution. It is clear to see the airspeed Mach number is closer to the desired value for higher mesh numbers in boundary layer section.

3.6. 3D CFD Analysis

After completing 2D CFD analysis for both cases, 3D CFD analysis of the geometries were performed. By considering computational capacity of the available hardware (work station computer), it becomes too hard to achieve the desired Y^+ values. So, by increasing the first layer thickness and providing a high-quality mesh, this analysis is done for higher Y^+ values. In next steps, the mesh number will be increased by decreasing the first layer thickness as shown in Table 3.5.1 and 3.5.2. Also, mesh convergence study is applied for these cases as well (see Figure 3.5.9 to Figure 3.5.12).

Table 3.6.1. Mesh statistics for 3D model for Mach 2

Mesh Number (million)	First Layer Thickness (m)	Growth Rate	Y^+ Value
4	2,00E-04	1,2	22,84
8	1,80E-04	1,16	20,18
12	1,30E-04	1,12	15,02
16	1,00E-04	1,10	11,5

As a results of 3D CFD analysis, Mach number distributions at the exit of the nozzle is satisfactory in terms of desired Mach number and boundary layer thickness as can be seen in following figures.

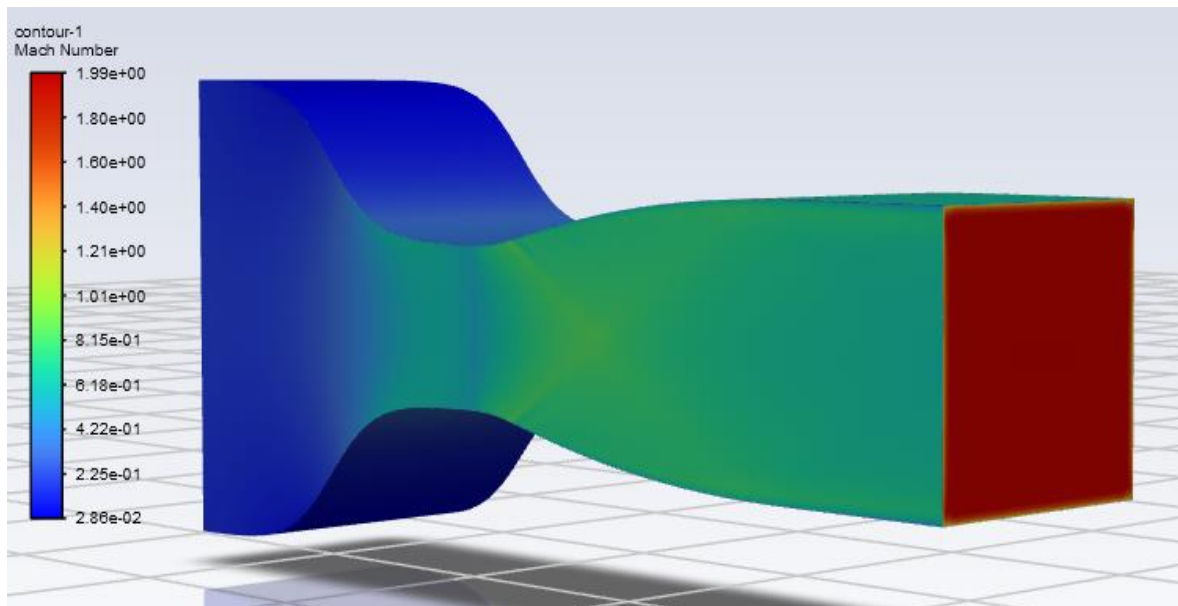


Figure 3.6.1. Mach number contours for 3D CFD analysis of Mach 2

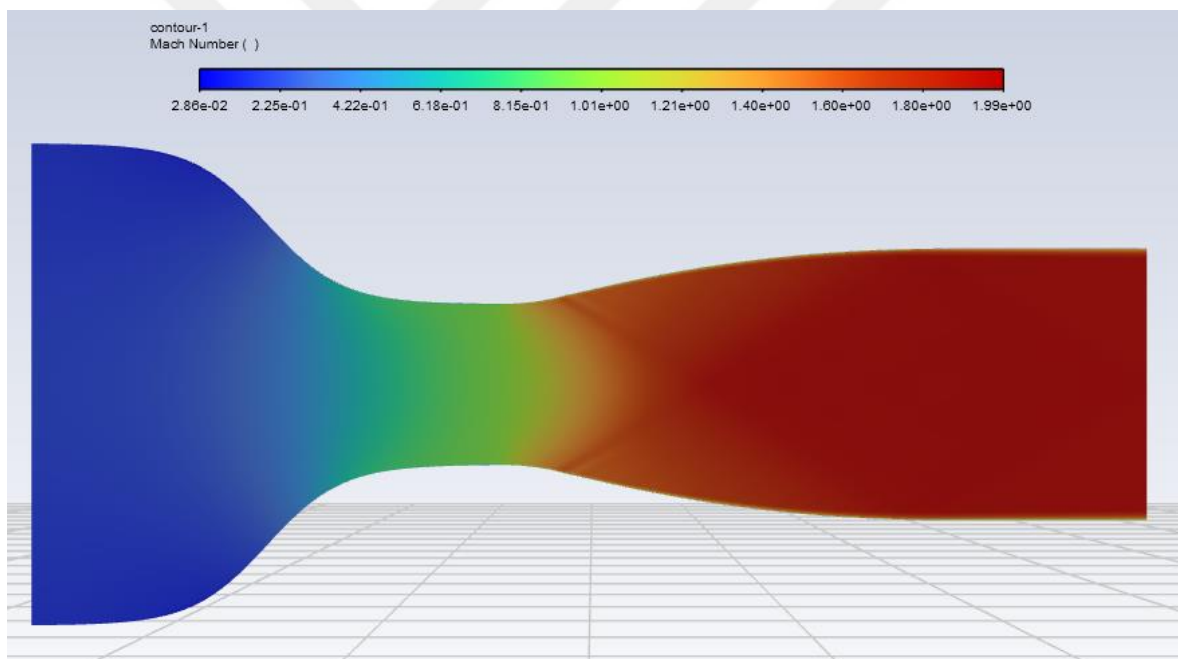


Figure 3.6.2. Mach number contours for 3D CFD analysis of Mach 2 (mid-plane)

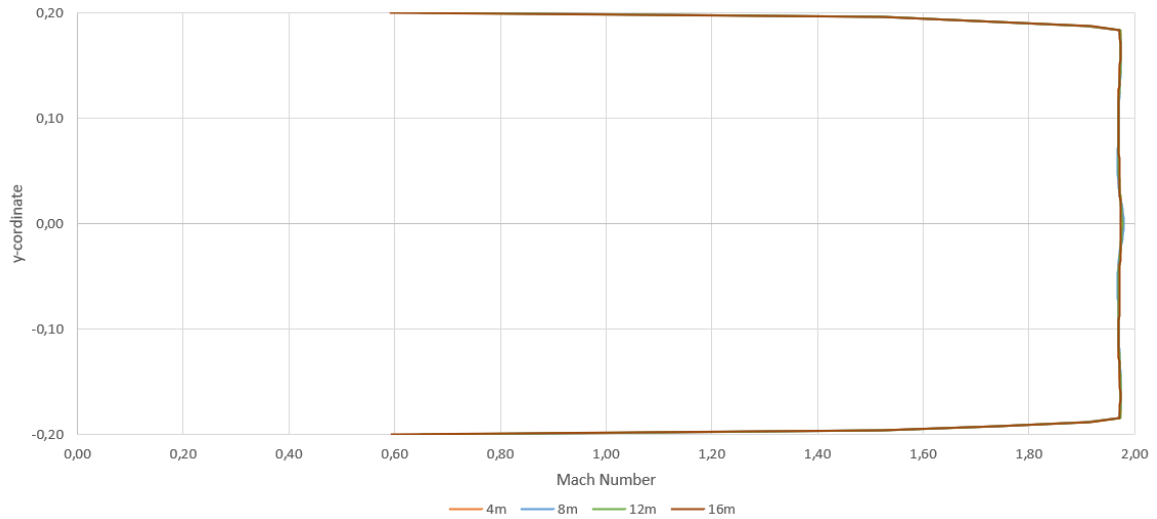


Figure 3.6.3. Mach number vertical distribution in the outlet of the nozzle for different mesh numbers (in millions) for 3D CFD analysis (2 Mach)

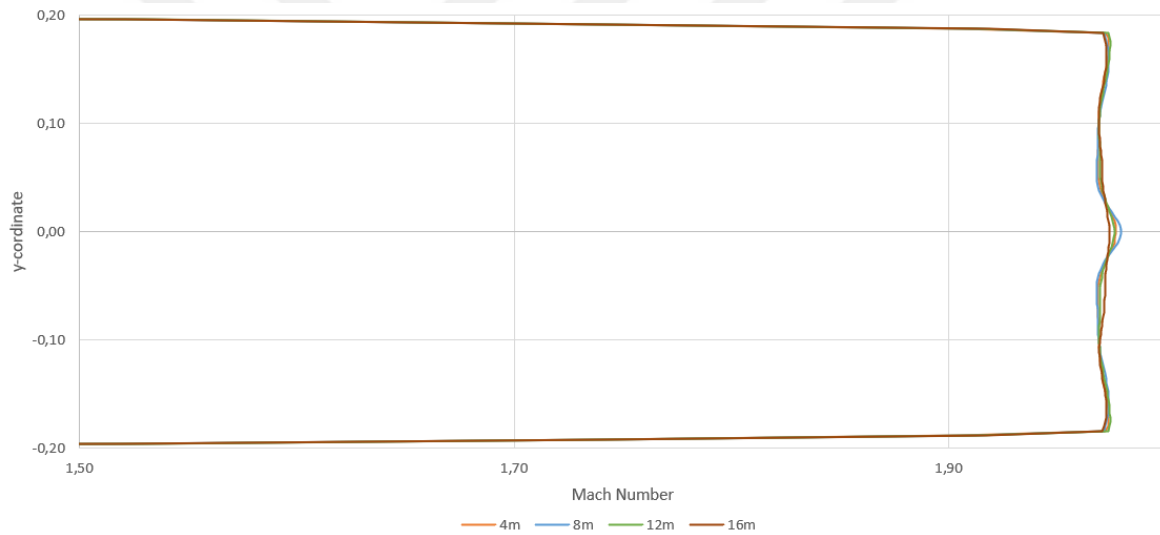


Figure 3.6.4. Mach number vertical distribution in the outlet of the nozzle for different mesh numbers (in millions) in a close range for 3D CFD analysis (2 Mach)

Table 3.6.2. Mesh statistics for 3D model for Mach 4

Mesh Number (million)	First Layer Thickness (m)	Growth Rate	Y+ Value
4	2,00E-03	1,2	232
8	1,60E-03	1,18	151
12	5,00E-04	1,17	71,1
18	1,00E-04	1,15	58,3

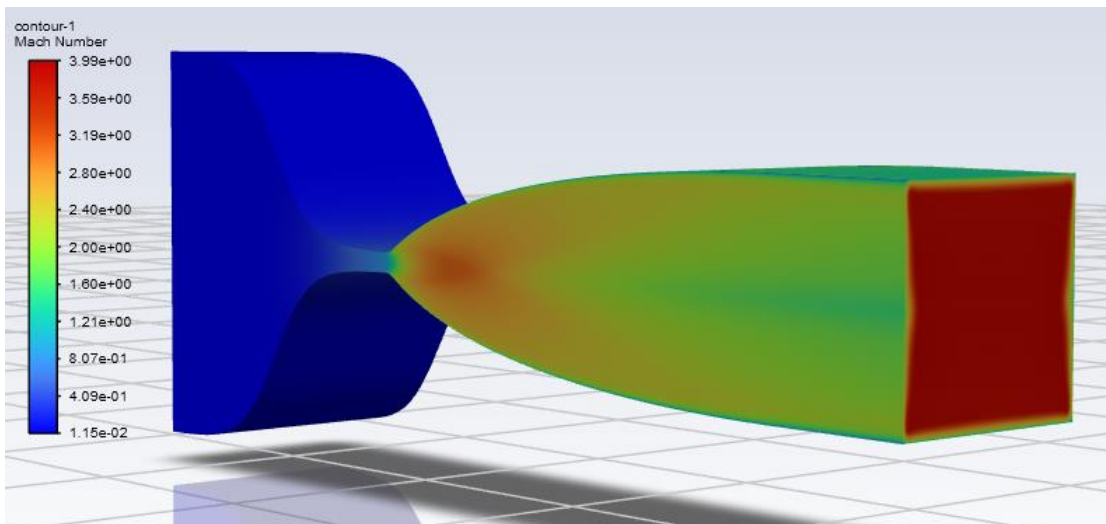


Figure 3.6.5. Mach number contours for 3D CFD analysis of Mach 4

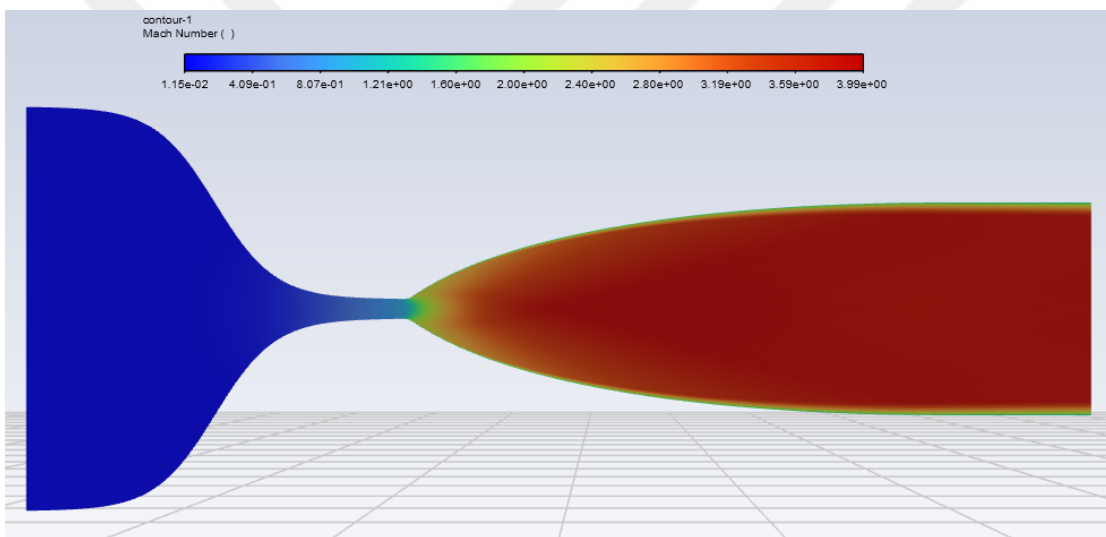


Figure 3.6.6. Mach number contours for 3D CFD analysis of Mach 4 (mid-plane)

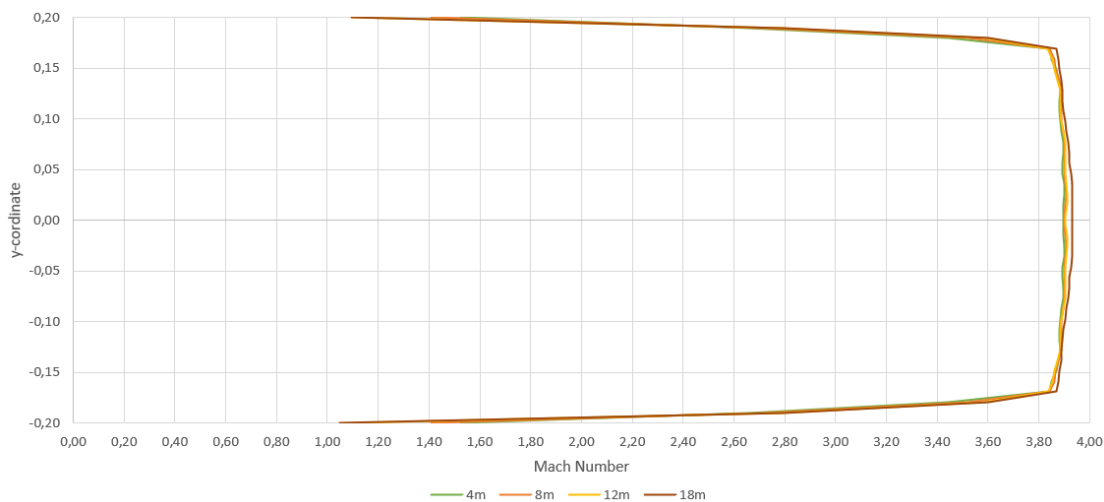


Figure 3.6.7. Mach number vertical distribution in the outlet of the nozzle for different mesh numbers (in millions) for 3D CFD analysis (4 Mach)

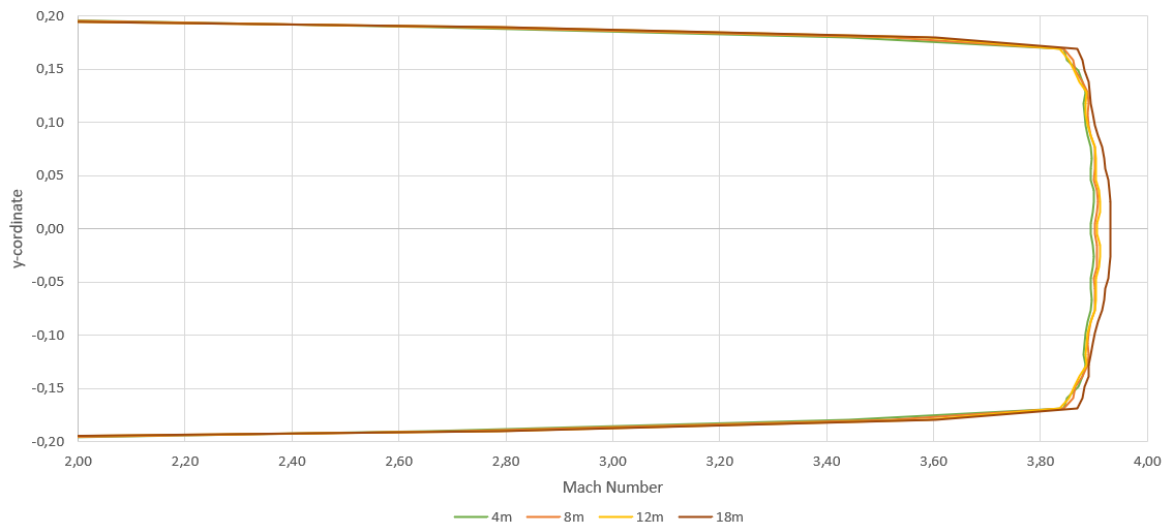


Figure 3.6.8. Mach number vertical distribution in the outlet of the nozzle for different mesh numbers (in millions) in a close range for 3D CFD analysis (4 Mach)

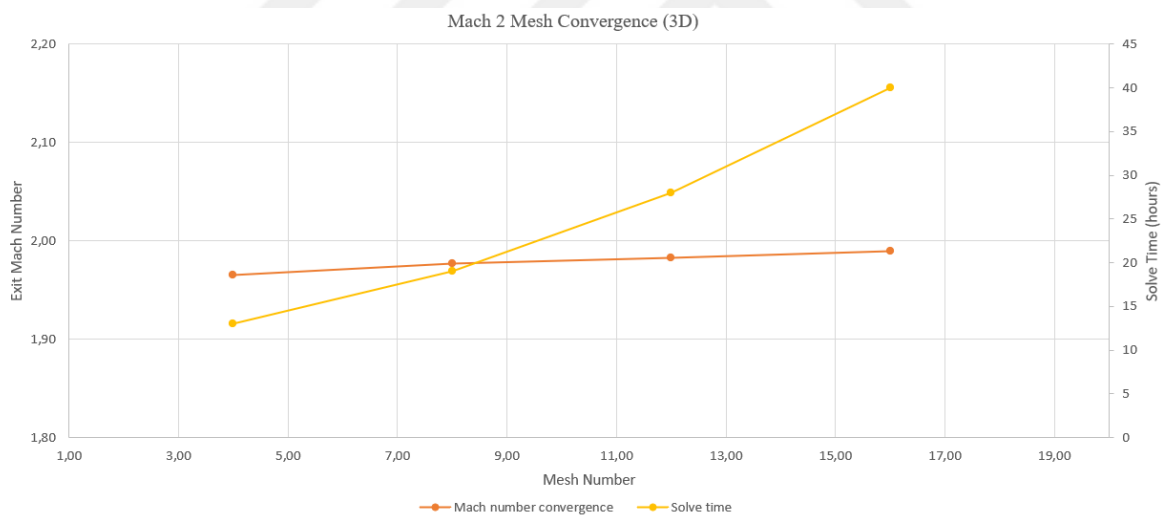


Figure 3.6.9. Mach 2 nozzle mesh convergence study (3d)

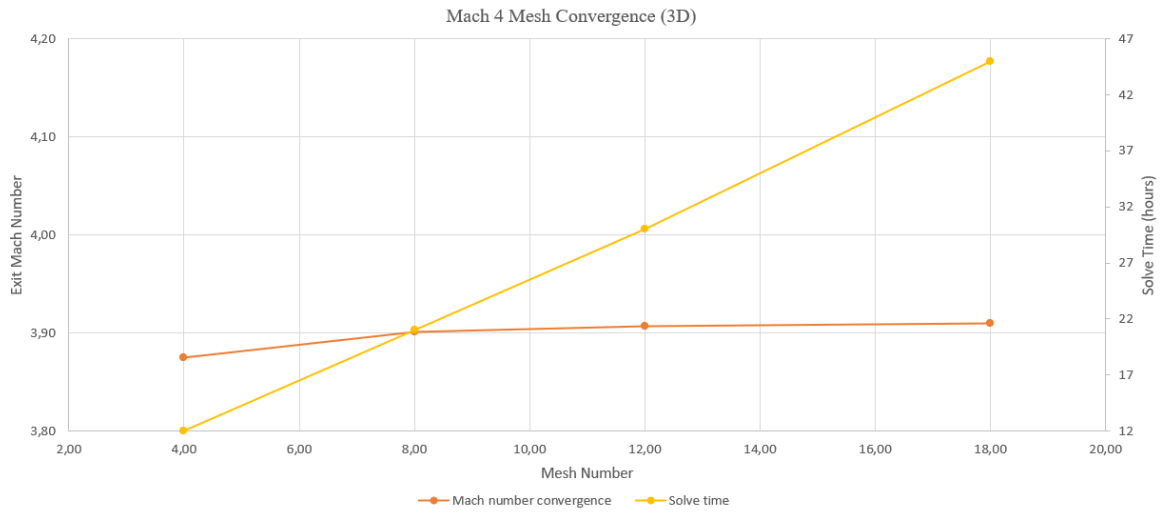


Figure 3.6.10. Mach 4 nozzle mesh convergence study (3d)

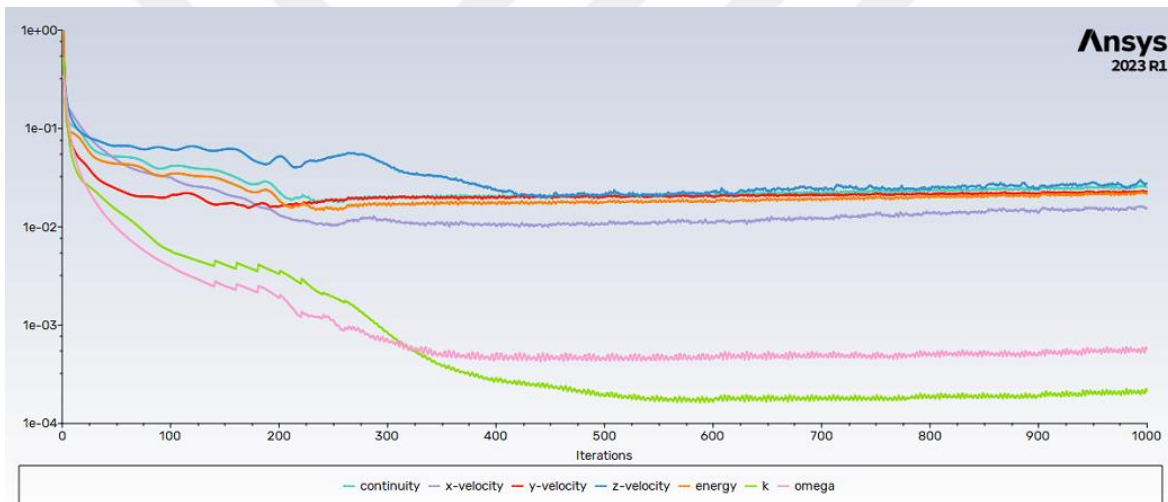


Figure 3.6.11. Mach 4 nozzle mesh convergence plot (3d – 12m mesh)

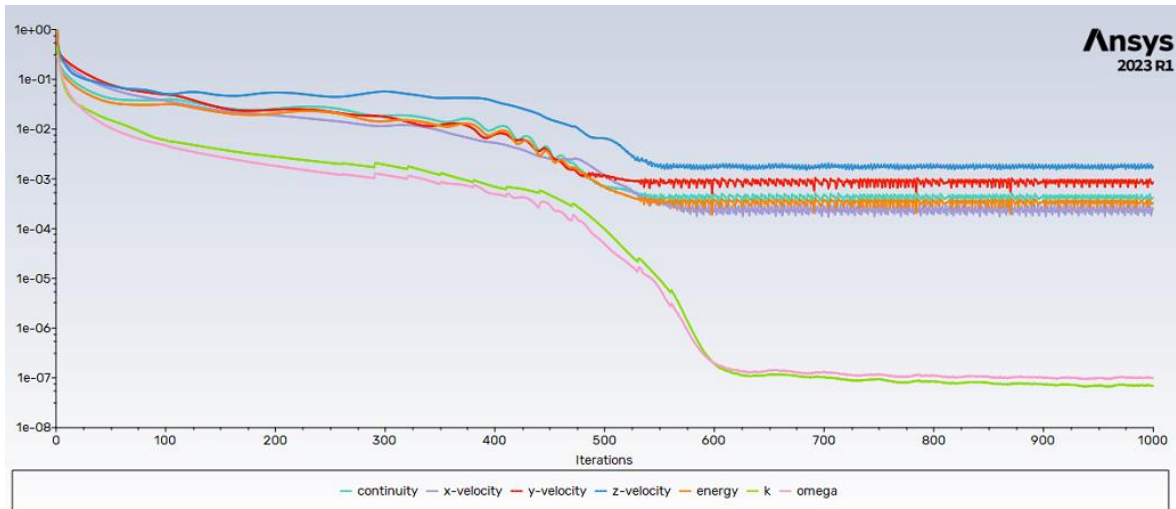


Figure 3.6.12. Mach 2 nozzle mesh convergence plot (3d – 8m mesh)

3.7. Comparison of 2D and 3D CFD Analysis

In this section of the study, 2D and 3D CFD analysis were compared. Results of the highest number of mesh analysis were used. The same boundary conditions were used on ANSYS Fluent 2023 R1.

As can be seen in Figure 3.6.1 and Figure 3.6.2, 2D analyses give different results than the 3D analyses due to the mesh quality depending on computational limits and increasing wall effects on 3D solution domain. The boundary layer thickness is lower for 3D analyses which sounds more promising.

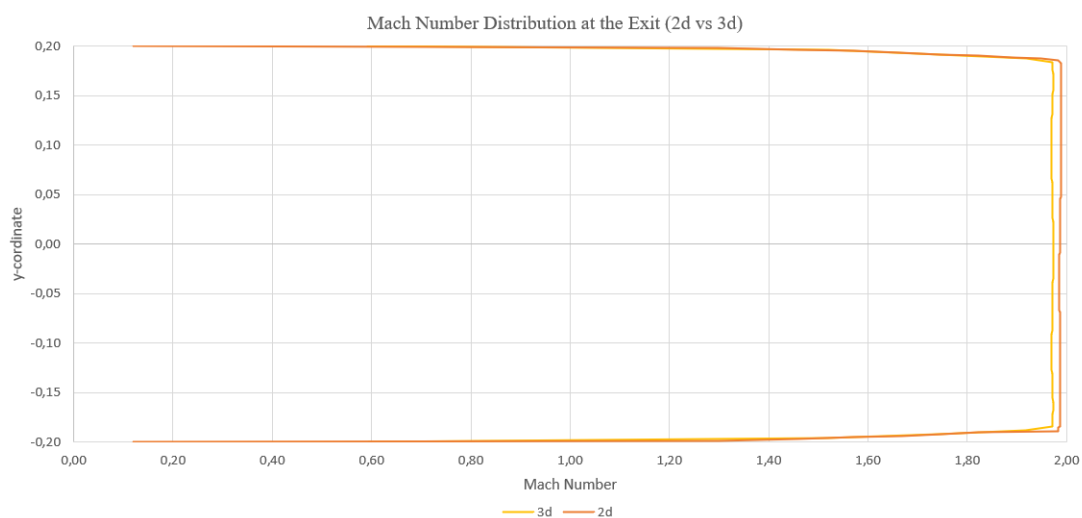


Figure 3.7.1. Comparison of 2D and 3D CFD analysis (Mach 2)

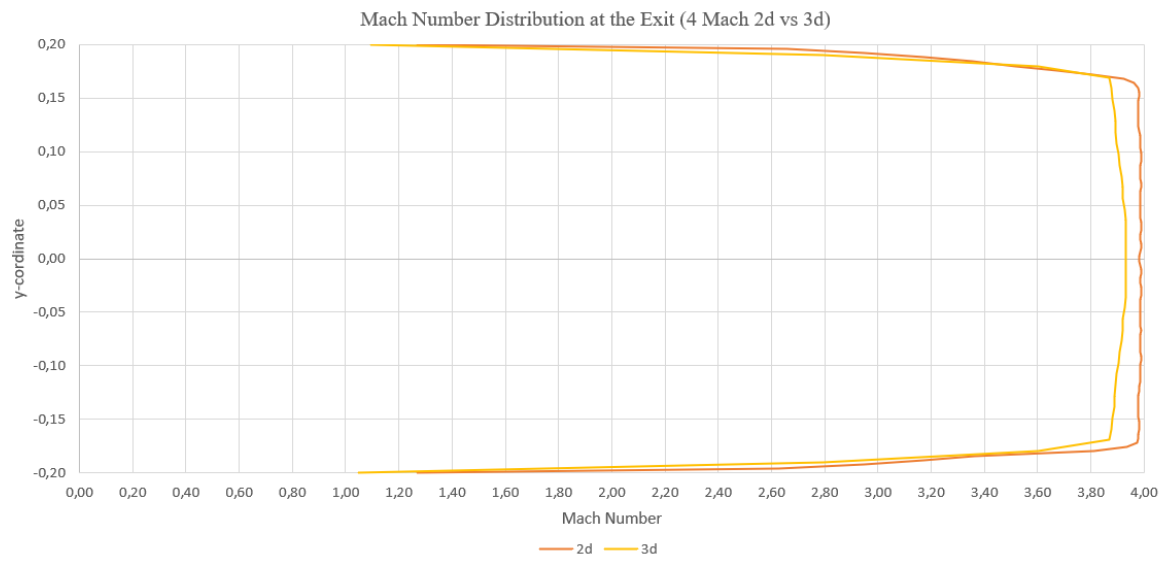


Figure 3.7.2. Comparison of 2D and 3D CFD analysis (Mach 4)

4. CONCLUSION

The preliminary design of an intermittent blow-down supersonic wind tunnel with maximum speed of Mach 4 is presented. Achieving desired parameters such as obtaining a Mach 4 maximum velocity in test section, running the system for 60 seconds, necessary calculations and assumptions were performed to obtain working conditions and nozzle and diffuser throat dimensions. The pressure ratios were specified by using isentropic flow properties. Pressurized air reservoir capacity was calculated depending on these parameters and run times of the tunnel with different Mach numbers (1.5 to 4) are calculated.

The most challenging part of this study was to obtain nozzle geometry. Researches on literature showed that the most common and accurate solution for this subject is Method of Characteristics. Method of characteristics (MoC) is useful numerical technique for resolving two-dimensional compressible flows evolution. This method allows the calculation of flow properties at various locations within the flow field, including direction and velocity. A MATLAB code derived to create desired nozzle geometry contour coordinates. To compare and validate the accuracy of the solution of Mach 4 nozzle, another case was created as Mach 2 nozzle and the whole operations mentioned above, were applied on the new case.

Coordinates of the nozzle boundary are imported to a CAD software, Solidworks. The test section's nozzle outlet is extended for half its length, where the model will be positioned. To control flow quality and evolution, Computational Fluid Dynamics (CFD) analysis was executed with ANSYS Fluent 2023 R1 program which has comprehensive modeling capabilities for a wide range of both turbulent and laminar compressible and incompressible fluid flow. As in that case, density-based solver is a more appropriate choice due to its capability of solving high-speed flow problems. The Shear Stress Transport turbulence model, $k - \omega SST$, was chosen for this case.

In order to obtain a more accurate solution, nozzle geometry was meshed obeying mesh quality criteria. Also, Y^+ estimation was done to specify wall distance of the mesh. For both 2D and 3D cases, appropriate Y^+ values were calculated by considering computational limits of available hardware.

To determine how responsive the simulation results are to adjustments in the mesh size or refinement, a mesh dependency analysis was conducted. In order to do this, the simulations were conducted at various mesh resolutions, and the effects of mesh refinement or coarsening were examined for both 2D and 3D analysis. With different mesh sizes, mesh metrics, flow uniformity, Y^+ values and Mach number distribution changes at the exit of the nozzle were compared.

Results from CFD analysis show that Mach number magnitude and its uniformity throughout the outlet boundary of the nozzle are satisfactory for both cases. Comparing with different mesh numbers of solution domains, proved that by increasing the mesh number (providing mesh quality within the limits) creates better solution. Mesh convergence study was conducted for all cases to compare relations between exit Mach numbers, mesh numbers and solving times. Also, a mesh dependence study applied and illustrated on boundary layer of the test section walls and results were satisfactory as well.

In terms of future works, these analyses should be performed utilizing a more capable hardware to acquire more accurate results especially for 3D solution as it enables to capture whole flow-field including corner flows of the nozzle.

REFERENCES

1. John D. Anderson, J. (2012). *Fundamentals of Aerodynamics (in SI units)*. In *The Aeronautical Journal* (Vol. 116, Issue 1176).
2. Anderson, J. D., *Modern Compressible Flows with Historical Perspective 3rd Edition*, McGraw-Hill Series in Aeronautical and Aerospace Engineering, 2003.
3. Pope, A., & Goin, K. L. (1965). *High-Speed Wind Tunnel Testing*.
4. Mehta R. D. (1977). The Aerodynamic Design of Blower Tunnels with Wide-Angle Diffusers, *Prog. Aerospace Sci.* vol. 18, pp. 59-120.
5. Bharath, B. K. (2015). Design and Fabrication of a Supersonic Wind Tunnel. *International Journal of Engineering and Applied Sciences*, 2(5).
6. Cattafesta, L., Bahr, C. and Mathew, J. (2010). Fundamentals of Wind-Tunnel Design. In *Encyclopedia of Aerospace Engineering* (eds R. Blockley and W. Shyy). <https://doi.org/10.1002/9780470686652.eae532>
7. Xia, Yu & Bruce, Paul. (2014). Tackling inflow conditions in experiment and computation. 10.13140/RG.2.2.12037.40162.
8. Zaheer, Syed & Disimile, Peter. (2022). Design and Parametric Analysis of a Mach 4 Wind Tunnel for SSLCs Studies. *Journal of Fluids Engineering*. 144. 10.1115/1.4054505.
9. M. A. Moelyadi, M. F. Izzaturrahman, C. Adnel, M. H. Izzuddin, E. Amalia; Design and CFD simulation of a compact supersonic wind tunnel. *AIP Conf. Proc.* 21 April 2020; 2226 (1): 020009.
10. Vallabh, B, & Skews, BW. (2017). Investigation of nozzle contours in the CSIR supersonic wind tunnel. *R&D Journal*, 33, 32-41. Retrieved February 09, 2024,
11. Pascual, J. (2007). Design of a supersonic wind tunnel. Mechanical Engineering Undergraduate Honors Theses Retrieved from <https://scholarworks.uark.edu/meeguht/21>
12. Kim S., Kim H., Kwon S., (2001). Transitional Behavior of a Supersonic Flow in a Two-dimensional Diffuser, *KSME International Journal*, Vol. 15, No. 12, pp. 1816-1821.
13. Pascual J. (2007), "Design of a supersonic wind tunnel" (2007). Mechanical Engineering Undergraduate Honors Theses. 21.
14. Fluent Theory Guide. (2013). Ansys Fluent Theory Guide. In ANSYS Inc., USA (Vol. 15317, Issue November, pp. 724–746).
15. Varner, M.O., Summers, W.E., Davis, M.W., "A Review of Two-Dimensional Nozzle Design Techniques", *AIAA 12th Aerodynamic Testing Conference*, 22-24 March 1982, Williamsburg, Virginia.

16. Ali, M. H., Mashud, M., Al Bari, A., & Islam, M. M. U. (2012). Numerical solution for the design of minimum length supersonic nozzle. *ARPJ Journal of Engineering and Applied Sciences*, 7(5), 605-612.
17. Göing M. (1990). Nozzle Design Optimization by Method-of-Characteristics, *AIAA 26th Joint Propulsion Conference*.
18. Khan, Md & Kumar, Sanjay & Sharath, M & Chowdary, Harika. (2013). Design of a Supersonic Nozzle using Method of Characteristics. *IJERT*.
19. Yen, Joseph C., and Martindale, William R., "An Inviscid Nozzle Design Approach to Perfect Flow Uniformity for Wind Tunnel Applications", *AIAA-2008-7059, 26th Applied Aerodynamics Conference*, 18-21 August 2008, Honolulu, Hawaii.
20. Prandtl, L. and Busemann, A. "Näherungsverfahren zur Zeichnerischen Ermittlung von Ebenen Stromungen mit Überschallgeschwindigkeit. *Stodola Festschrift (Zurich)*, 1929, S. 499-509.
21. Sivells, J.C., "A Computer Program for the Aerodynamic Design of Axisymmetric and Planar Nozzles for Supersonic and Hypersonic Wind Tunnels", *AEDC-TR-78-63*, Dec. 1978.
22. Adams, S. E. (2016). The Design and Computational Validation of a Mach 3 Wind Tunnel Nozzle Contour.
23. Shope, Fredrick L., "Contour Design Techniques for Super/Hypersonic Wind Tunnel Nozzles", *AIAA-2006-3665, 24th Applied Aerodynamics Conference*, 5-8 June 2006, San Francisco, California.
24. Pettersson K. Scaling techniques using CFD and wind tunnel measurements for use in aircraft design. Licentiate Thesis, KTH. Thesis number: 64, 2006.
25. Hodge, B.K., and Koenig, Keith, *Compressible Fluid Dynamics with Personal Computer Application*, Prentice Hall, New Jersey, 1995.
26. Moonen P, Blocken B, Carmeliet J. Indicators for the evaluation of wind tunnel test section flow quality and application to a numerical closed-circuit wind tunnel. *International Journal of Wind Engineering and Industrial Aerodynamics*. 2007; 95: 1289-1314.

ÖZGEÇMİŞ

Kişisel Bilgiler

Soyadı, adı : K*****, K**** G****
Uyruğu : T.C.
Doğum tarihi ve yeri :
Medeni hali :
Telefon : 0
e-mail :

Eğitim

Derece	Eğitim Birimi	Mezuniyet Tarihi
Yüksek lisans	SBTÜ/ Savunma Teknolojileri	Devam ediyor
Lisans	Gaziantep Üniversitesi / Uçak ve Uzay Mühendisliği	2019
Lise	Şehremini Anadolu Lisesi	2014

İş Deneyimi

Yıl	Yer	Görev
2020-Halen	Sivas Bilim ve Teknoloji Üniversitesi	Araştırma Görevlisi

Yabancı Dil

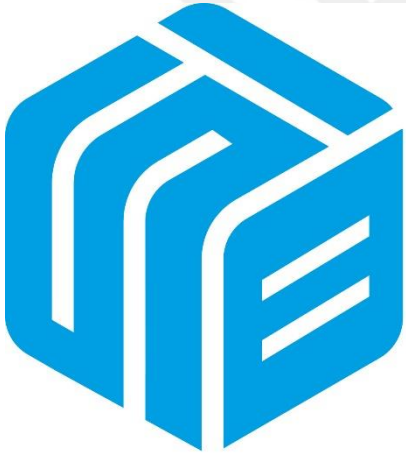
İngilizce

Yayınlar

Preliminary Design Of A Mid-Scale Supersonic Wind Tunnel, *Ankara International Aerospace Conference, AIAC-2021-125.*

Hobiler

Müzik, Sinema, Spor



**SIVAS
BİLİM VE TEKNOLOJİ
ÜNİVERSİTESİ**

KÖKLERDEN GÖKLERE...